Pleistocene-Holocene tectonic reconstruction of the Ballık travertine (Denizli Graben, SW Turkey): (De)formation of large travertine geobodies at intersecting grabens

Koen Van Noten[a,b,*], Savaş Topal[c], M. Oruç Baykara[c], Mehmet Özkul[c], Hannes Claes[d,1], Cihan Aratman[c,d], Rudy Swennen[d,**]

[a] Seismology-Gravimetry, Royal Observatory of Belgium, Ringlaan 3, 1180 Brussels, Belgium
[b] Geological Survey of Belgium, Royal Belgian Institute of Natural Sciences, Jennerstraat 13, 1000 Brussels, Belgium
[c] Department of Geological Engineering, Pamukkale University, 20070, Kınıklı Campus, Denizli, Turkey
[d] Geodynamics and Geofluids Research Group, Department of Earth and Environmental Sciences, Katholieke Universiteit Leuven, Celestijnenlaan 200E, 3001 Leuven, Belgium

A B S T R A C T

Travertine geobodies have been identified as potential reservoir analogues to carbonate build-ups in pre-salt hydrocarbon systems. To investigate travertine geobody deformation, faults were mapped in 35 travertine quarries that excavate the Ballık travertine, i.e. a c. 12.5 km^2 large travertine geobody that precipitated at the intersection of the NE margin of the Denizli Basin and neighbouring Baklan Graben (SW Turkey). This travertine precipitated from cooling carbonate-saturated thermal spring waters that resurfaced along the margin fracture/fault network and through Neogene unconsolidated underlying sediments. From the Denizli basin floor to the uplifted graben shoulders, fault orientation is dominantly WNW-ESE oriented with major basin faults showing a left-stepping trend. Along the upper Denizli margin, travertine is only deformed by extensional normal faults. Along the lower margin, travertine starts with a subhorizontal facies but evolves to a travertine facies formed by a sloping topography with a domal architecture. Paleostress inversion of fault-slip data reveals that an Early Pleistocene NNE-SSW extensional-transtensional phase initiated the WNW-ESE oriented, graben-facing normal fault network. In the Middle Pleistocene, the Ballık fault network was left-lateral strike-slip reactivated because it acted as a transfer zone between the NW-SE extending neighbouring Baklan Basin and NW-SE extension along NE-SW oriented margin faults of the DGHS. In this stress configuration, travertine precipitated along the SW margin fault of the Baklan Graben. After strike-slip reactivation, a Late Pleistocene-to-current NNE-SSW extensional stress regime reinstalled during which margin faults widened and active travertine precipitation moved to more central parts of the DGHS. As different tectonic regimes affect graben intersections, reservoir analogues can have a complex deformation history driven by fault reactivation and recurrent stress permutations. This study concludes that large travertine geobodies can form at graben intersections because of their susceptibility to enhanced fluid flow through the complex fault-fracture network.

1. Introduction

In situ reservoir characterisation is most often based on the combination of seismic and core data. In particular for complex carbonate reservoirs, the sedimentological and tectonic features between core and seismic-scale are decisive for production. Outcrop analogue studies cover this scale-gap and their integration is thus indispensable in multidisciplinary complex carbonate reservoir characterisation. Most carbonate reservoirs are naturally fractured from micro- to kilometre scale with fractures acting as highways for fluids in the reservoir, or enhancing compartmentalisation after cementation. A proper understanding of the reservoir-scale fracturing behaviour is essential for reservoir characterisation. Among continental carbonate reservoir analogues, travertines best represent the close interaction between

---

* Corresponding author. Seismology-Gravimetry, Royal Observatory of Belgium, Ringlaan 3, 1180 Brussels, Belgium.
** Corresponding author.
E-mail addresses: koen.vannoten@seismology.be (K. Van Noten), rudy.swennen@kuleuven.be (R. Swennen).
[1] Now at Clay and Interface Mineralogy, Energy & Mineral Resources, RWTH Aachen University, Bunsenstrasse 8, 52072 Aachen, Germany.

sedimentation, crustal fluid circulation and, especially, neotectonic deformation in actively deforming tectonic regions (Hancock et al., 1999). Travertine morphology or reservoir architecture is controlled by paleo-topography. The latter itself is, however, strongly dependent on regional and local faulting, affecting spring water discharge and spring orifices that generated the necessary slopes to allow superficial fluid flow. Travertines can be valuable tectonic archives. To properly interpret sedimentological analyses and reconstruct complex travertine build-ups, a detailed structural analysis, in which tectonic tilting is addressed, always needs to accompany travertine sedimentology. Structural analysis moreover allows revealing the presence of the fault-fracture network in the subsurface that provided the necessary fluid pathways.

In actively deforming regions, faults control the occurrence, size and geometry of travertine deposits. Geometrically, travertines occur as isolated individual elongate fissure ridges and as (large) travertine geobodies deposited in flat pools or as slope-controlled travertine mounds. Whereas travertine growth along fissure ridges is considered to develop episodically (e.g. Mesci et al., 2008), with fluid expulsion and fissure propagation being impacted by earthquake activity (Brogi and Capezzuoli, 2014), large-scale travertine depositions can last for several thousands of years, being fed by an actively enhanced fault-fracture network. Structurally, travertines develop in the fractured hangingwall of normal faults (Altunel, 1994; Brogi, 2004; Brogi and Capezzuoli, 2009, 2014; Brogi et al., 2010; Özkul et al., 2014), in shear zones (Faccenna, 1994; Faccenna et al., 2008), above fault tips or near their lateral end (Çakır, 1999; Kele et al., 2008), but the largest masses can develop in strain-releasing step-overs and along relay ramps developed between margin-bounding faults (Altunel and Hancock, 1993b; Çakır, 1999; Hancock et al., 1999; Martínez-Díaz and Hernández-Enrile, 2001; Brogi et al., 2012; Temiz et al., 2013). Not only the travertine outline reveals the geometry of the underlying fault system, also systematic joints and faults cutting through the travertine can be used as stress indicators for the reconstruction of contemporary tectonic stress field that has affected the travertine area, either during or after deposition (Altunel, 1994; Kaymakçı, 2006). Joint propagation and morphology is hereby strongly influenced by the internal heterogeneity of the travertine (Hancock et al., 1999; Van Noten et al., 2013).

Travertine occurrences in the Denizli Graben-Horst System (DGHS, Koçyiğit, 2005) in the West Anatolian Extensional Province (WAEP, southwest Turkey; Fig. 1A and B) are one of the best studied around the world. In the DGHS, the most famous travertine exposure is located at the Hierapolis-Pamukkale UNESCO world heritage site (https://whc.unesco.org/en/list/1545), where travertine is actively precipitating along the Pamukkale Fault Zone. In the Pamukkale area, fault, fracture and fissure mapping and their relationship to seismic activity has been studied to link travertine deposition to the neotectonic context of the Denizli area (Altunel and Hancock, 1993b,a, 1996; Hancock et al., 1999; Özkul et al., 2002; Koçyiğit, 2005; Kaymakçı, 2006; De Filippis et al., 2012; De Filippis et al., 2013; Özkul et al., 2013; Brogi et al., 2014).

Recently, the large-scale Pleistocene Ballık travertine geobody, c. 12.5 km², which deposited along the north-eastern step-like faulted northern margin of the DGHS (Fig. 1C), received much attention as reservoir analogue. In this region, travertines are both present along the uplifted margin flank and at the foot of the margin where they are exposed in a large, 2 km-long, ~70 m high, travertine domal structure (further referred to as the *Killik dome*) that developed on top of the ancient Neogene and Pleistocene basin fill. The fact that this domal structure resembles to carbonate build-ups in Pre-Salt plays offshore Brazil (Buckley et al., 2013), in the Namibe Basin (Sharp et al., 2013) and offshore Angola (Saller et al., 2016) was the reason to study the Ballık travertine as a reservoir analogue (Claes et al., 2015; De Boever et al., 2016).

Along the northern and southern margin of the DGHS, margin-bounding faults are mostly characteristic of pure normal faulting or

normal faulting with a small oblique-slip component (Altunel, 1994; Çakır, 1999; Koçyiğit, 2005; Kaymakçı, 2006). Uncommon with respect to other margin-bounding faults or to focal mechanisms of recent earthquakes (Irmak, 2013), many purely strike-slip kinematic markers are present in the fault infill in the Killik dome (Van Noten et al., 2013). However, strike-slip faulting is very rare in the DGHS. Altunel (1994) reported sinistral strike-slip faults offsetting man-made channels and structures at Hierapolis (Pamukkale) and a few minor WNW-striking strike-slip faults cutting through the fissure ridge at Koçabas. Van Noten et al. (2013) interpreted strike-slip faulting affecting the Killik dome to have occurred during a transient strike-slip stress field in the Pleistocene hereby reactivating the already existing normal faults. However, to date any link with a larger-scale regional tectonic model and the scale of strike-slip reactivation is lacking and needs to be addressed.

With the aim of understanding the tectonic evolution of the entire north-eastern graben flank of the Ballık area, a detailed structural analysis of the Ballık travertine is presented in this study. As travertines are heavily quarried in this area and evidences will be progressively removed in the near future, it is essential to document and report all structural features along this graben flank. This study focuses on the orientation of major travertine structures and domes, and on fault orientation and fault-slip kinematic data. After a geometric analysis on the observed faults, a paleostress analysis is performed on the collected kinematic data. The resulting paleostress directions allow deducing if stress variations occurred during the deformation of the entire NE margin of the DGHS. The dip and orientation of the different travertine masses are only briefly described as a detailed facies analysis is beyond the scope of the study. This study provides an overview of tectonic structures that overprinted the travertine geobodies which provides a tectonic framework for further studies that focus on facies analysis, geochemistry and sedimentology of the Ballık travertine from which the travertine geobody architecture can be reconstructed.

2. Tectonic framework

2.1. Turkey geodynamics

The DGHS is a seismically active basin situated in the West Anatolian Extensional Province (WAEP) in SW Turkey (Fig. 1A). The WAEP developed from a complex interaction of large-scale plate tectonics in the Aegean and Anatolian areas. Due to northwards migration of the Arabian Plate, on the one hand, and the northwards roll-back subduction of the African Plate below the Anatolian Plate in the Aegean region, on the other hand, an anticlockwise rotation and a westwards squeeze-out motion affected the Anatolian plate (Fig. 1A) (McKenzie, 1970; Seyítoğlu and Scott, 1996; Westaway et al., 2005; Alçiçek et al., 2007; ten Veen et al., 2009; van Hinsbergen et al., 2010; Gessner et al., 2013). Tectonic relaxation resulted in the development of a pronounced extensional stress regime in West Anatolia as shown by the predominantly NE-SW to NW-SE trending grabens, cross-grabens and horst-graben structures developed from the Pliocene to the Quaternary (Westaway, 1993; Seyítoğlu and Scott, 1996; Bozkurt, 2001; ten Veen et al., 2009). Most of these margin-bounding seismogenic faults, including the Denizli margin faults, are still active and were responsible for a number of devastating earthquakes in historic and recent times (Taymaz and Price, 1992; Irmak and Taymaz, 2009; Irmak, 2013). The development and destruction of numerous ancient cities in the Denizli area was affected significantly by destructive earthquakes (estimated > M6) (Piccardi, 2007). Continuous earthquake activity along the margin faults has affected the Pliocene to recent deposits near the margin as well as the poorly-lithified Quaternary sediments in the basin creating typical earthquake-related soft-sediment deformation structures (Topal and Özkul, 2014).

In the Menderes Massif, geothermal areas are abundant. They represent hydrothermal flow systems in the crust and are closely related to crustal extension, magmatic activity and surface uplift (Gessner
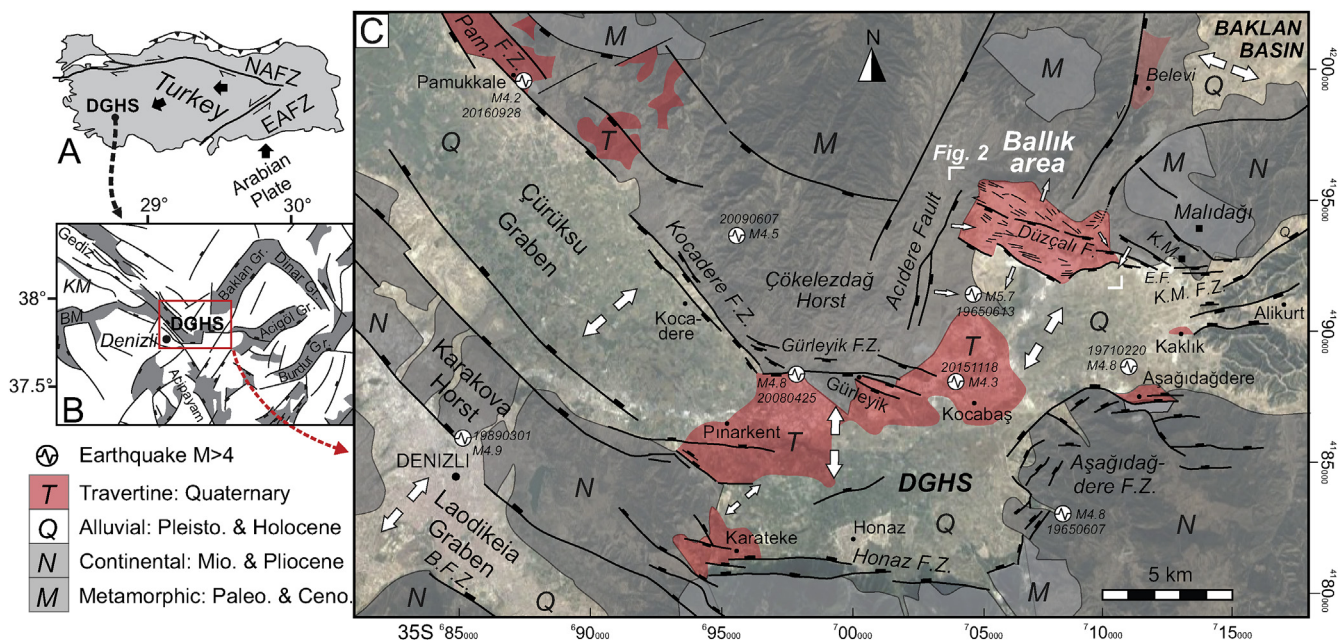
Fig. 1. A) Location of the Denizli Graben-Host System (DGHS) in Turkey. NAFZ: North Anatolian Fault Zone, EAFZ: East Anatolian Fault Zone. **B)** Sedimentary basins in the West Anatolian Extensional Province. BM = Büyük Menderes Graben; KM: Küçük Menderes Graben. **C)** Fault map of the eastern DGHS. Faults are derived from geomorphology and from Koçyiğit (2005). The Ballık study area is located along the northern graben flank in the eastern part of the DGHS. Minor faults drawn in the Ballık area are discussed in this study. Location of the M5.7 13 June 1965 earthquake is taken from Westaway (1993), other earthquakes are taken from the USGS Earthquake catalogue. K.M.: Küyükmalı Mountain; E.F.: Elmalı fault. B.F.Z.: Babadağ Fault Zone. Map coordinates are in UTM 35S, WGS 84. Basemap © Google Earth™.

et al., 2017). Hydrothermal fluid circulation is especially enlarged at graben-bounding normal fault zones, where brittle failure provided key pathways for meteoric and deep groundwater fluid flow (Güleç et al., 2002; Brogi et al., 2016). Especially at local graben fault intersections, enhanced fluid flow occurs and large geothermal fields are found (Faulds et al., 2009).

2.2. The Denizli Graben-Horst System

The DGHS is surrounded by the E-W trending Gediz, Küçük Menderes and Büyük Menderes Grabens in the east, the NW-SE Acıpayam Graben in the south and the Baklan Graben in the northeast (Westaway, 1990, 1993; Price and Scott, 1994; Koçyiğit, 2005; Kaymakçı, 2006) (Fig. 1B). High-angle normal faults, expressed as steep topographic scarps, delimit these basins. Many of these conjugate graben systems are consistent with a NE-SW, NW-SE and N-S multi-directional extension (Bozkurt and Sözbilir, 2006; Gürbüz et al., 2012). The horst-graben morphology of the DGHS formed during alternating seismic periods of subsidence and tectonic uplift (Westaway et al., 2005). A full description of the successive lithologies from the Miocene to recent Quaternary alluvial plain basin and travertine deposits can be found in Alçiçek et al. (2007) and Claes et al. (2015).

The NW-SE oriented western and central part of the DGHS can be separated into two Quaternary subgrabens, namely the Çürüksu and Laodikeia Subgrabens, separated by the uplifted Karakova Horst (Kaymakçı, 2006; Topal and Özkul, 2014). The Çürüksu Subbasin forms a c. 50 km long basin that is bordered by the Pamukkale normal fault zone in the northeast (Fig. 1B). Along this fault zone several travertine deposits, among which the active UNESCO Pamukkale travertines, are precipitated in kilometre-wide, left-lateral step-over zones that are developed at the end or between different segments of NW-SE-trending normal margin faults (Altunel and Hancock, 1993b; Çakır, 1999; Hancock et al., 1999). Along the northern margin, travertine occurrences are present as complex travertine mounds (Altunel and Hancock, 1993a,b; Kele et al., 2011; Özkul et al., 2013) and as small individual

fissure ridges which developed above different branches or step-overs of the NW-oriented margin faults (Altunel and Karabacak, 2005; De Filippis et al., 2012, 2013; Özkul et al., 2013; Yalçiner, 2013; Brogi et al., 2014).

The Ballık study area is situated at the south-eastern end of the DGHS where the basin morphology changes from NW-SE to locally E-W, forming the lateral extend of the Acigöl Graben in the east. This part of the DGHS has a pronounced staircase geometry. The southern border is delimited by the E-W graben-facing, step-like Honaz fault zone that is separated from the Babadağ fault zone by the NW-oriented transfer zone at Karateke (Fig. 1C). The Honaz fault zone is dominated by normal to oblique-slip faults along which slickenlines all point towards the centre of the basin, indicative of differential extension rate (Topal, 2012; Özkaymak, 2015). The Aşağıdağdere fault zone is situated at the most southeastern edge of the DGHS and consists of several short, closely-spaced fault segments that are dominated by oblique-slip normal faults (Koçyiğit, 2005). Along the northern margin, the NW-trending Kocadere fault zone is considered to be the prolongation of the Pamukkale fault zone (Fig. 1C). The short E-W to WNW-ESE normal faults NE of Pınarkent belong to the Gürleyik fault zone and mark the transition from the NW-SE trending to the E-W trending orientation part of the DGHS. It is unknown if these smaller faults continue and maintain their trend towards the WNW-ESE oriented travertine fissure ridge at Kocabaş (Hancock et al., 1999; Özkul et al., 2002; Altunel and Karabacak, 2005; De Filippis et al., 2012).

Between Kocabaş and the Ballık area, the DGHS has a NW-SE to ENE-WSW orientation (Fig. 2). In the west, this subbasin is bounded by the N-S Acıdere fault which separates the flat Denizli basin floor in the east from the uplifted Çökelezdağ Horst in the west. The Ballık area is situated along the northern margin and is characterised by several closely-spaced, mainly WNW-ESE faults that are mapped and addressed in detail in this study. NE of the study area, the eastern margin fault of the Baklan Graben intersects with the DGHS.
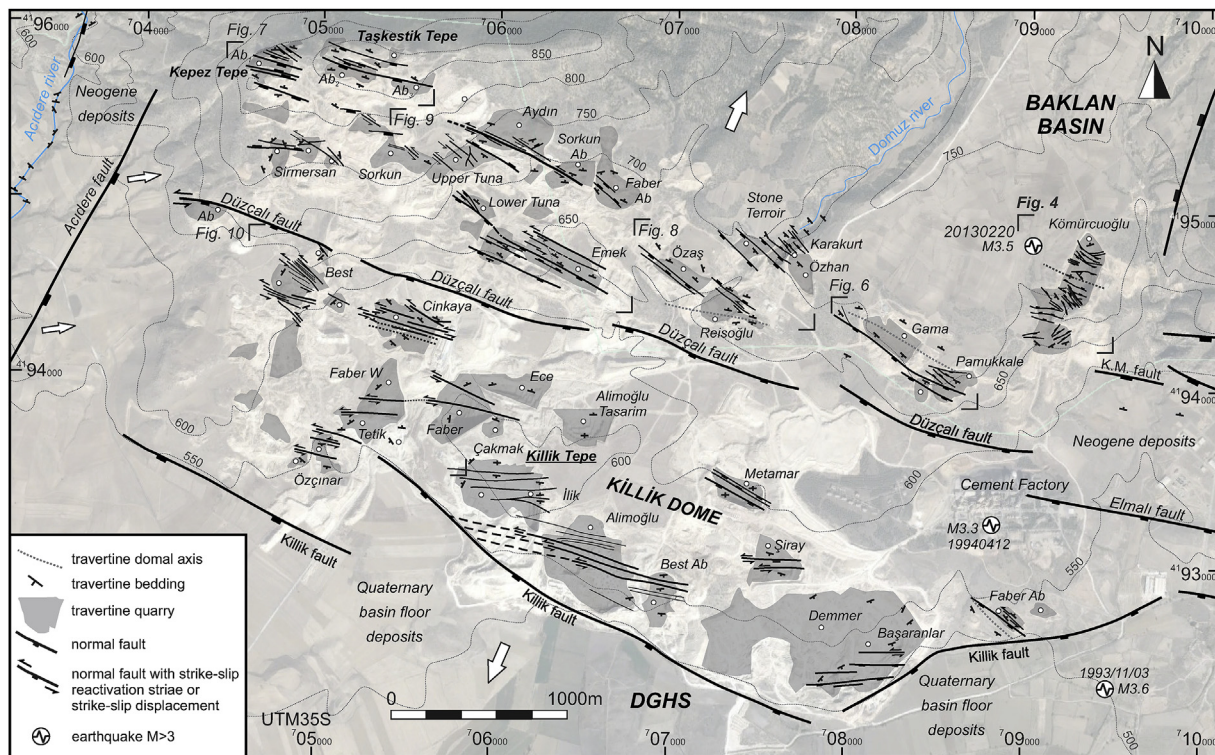
116

Fig. 2. Ballık fault map. Grey areas outline the studied quarries and excavation fronts in 2013 (basemap © Google Earth). Coordinates are in UTM 35S. Eye altitude of satellite image is 5.07 km. The Düzçalı fault segments and the large normal faults bordering the travertine excavation area are derived from geomorphology and after Koçyiğit (2005). Topographic isohypses are taken from the 1:25 000 Denizli M22-B1-B4 topographic maps (1989) illustrating the original topography before excavation of the northern flank. White dots = quarries; Ab = Abandoned quarry; K.M. (F.Z.) = Küçükmalıdağ (Fault Zone).

2.3. Travertine of the Ballık area

The mountain range front at Ballık, situated 25 km ENE from the city of Denizli, can clearly be recognised on ASTER satellite images, SRTM DEM and Google Earth™ images (see kml in Suppl. Mat. S1). The Ballık area forms a steep hill which starts at a basin floor altitude of c. 500 m asl. and reaches a maximum height of 877 m in the west at the Taşkestik Tepe (Fig. 2), i.e. 377 m above the current Denizli basin floor resulting from systematic Quaternary uplift. From top to bottom along the graben flank, travertine deposits are exposed along stepped, SW-, graben-facing slopes. 35 quarries that have excavated this large area are addressed in this study. The Ballık travertine, also referred to as the eroded-sheet travertines (sensu Altunel, 1994) or Kocabaş travertine geobody (Hancock et al., 1999; Khatib et al., 2014; Lebatard et al., 2014), is by far the largest travertine site in southwest Turkey (12.5 km²) with travertine thickness up to at least 120 m (Özkul et al., 2013). The Ballık travertine has been widely used around the world since ancient times as a construction stone due to its good mechanical resistance and durability properties (Çobanoğlu and Çelik, 2012; Çelik et al., 2014).

Based on the morphology of the northern graben flank, a northern upper margin area can be separated from the Killik dome. The quarries excavating the Killik dome, i.e. the Faber, Ece, Tetik, Çakmak, İlik, Alimoğlu and Best abandoned (abandoned is further noted as *Ab.*) quarries (see Fig. 2 and kml in Suppl. Mat. S1 for location of the quarries), were already the subject of several sedimentological and geochemical (Özkul et al., 2013; Khatib et al., 2014; Claes et al., 2015, 2017b; El Desouky et al., 2015; De Boever et al., 2017), geomechanical (Çobanoğlu and Çelik, 2012; Çelik et al., 2014), dating (Lebatard et al., 2014), petrophysical (Soete et al., 2015; De Boever et al., 2016) and structural (Van Noten et al., 2013) studies. The Killik dome is characterised by horizontally bedded travertine at its base that gradually changes upwards into complex, slope travertines that are dominated by

biohermal reed, cascade and waterfall travertine facies (Özkul et al., 2013; Claes et al., 2015; De Boever et al., 2017). Travertines precipitated from resurfaced meteoric waters that infiltrated along the margin that was already affected by a fault-fracture network. Fluids emerged as heated geothermal waters along the margin faults after having migrated through and interacted with the Lycian basement rocks (Claes et al., 2015; El Desouky et al., 2015). In a later stage, secondary fluid circulation was established with meteoric water interacting at depth and precipitated as calcite veins grown in faults and in the solution-enlarged fracture network cutting the travertine (Van Noten et al., 2013; El Desouky et al., 2015).

Travertines are thus not only restricted to the Killik dome (Fig. 2) but dominate the entire north-eastern upper graben flank of the DGHS. East and west of the Killik dome, travertine sequences consist mostly of subhorizontal bedded travertine that laterally extends for a few hundreds of meters. Also along the northern flank many lateral intercalations of fluvial conglomerate, sandstone, mudstone, paleosol horizons and erosional surfaces occur (Özkul et al., 2002). Altunel (1994) was the first to study the faults cutting the upper graben flank. Although the travertine masses along the margin flank constitute the largest part of the Ballık area and are intensively quarried, they hardly received any attention after Altunel's pioneering study and a detailed fault mapping and tectonic analysis of the entire NE Denizli graben flank was never performed.

3. Methodology

The northern graben flank was investigated during an extensive field campaign in 2014 and revisits in 2015 and 2016. Our study focuses on brittle structures such as joints (barren fractures without any slip), open fissures (no displacement and infill), faults and fault kinematic indicators including slickensides, slickenlines and displaced travertine lamination and paleosols. The orientation of planar structures is
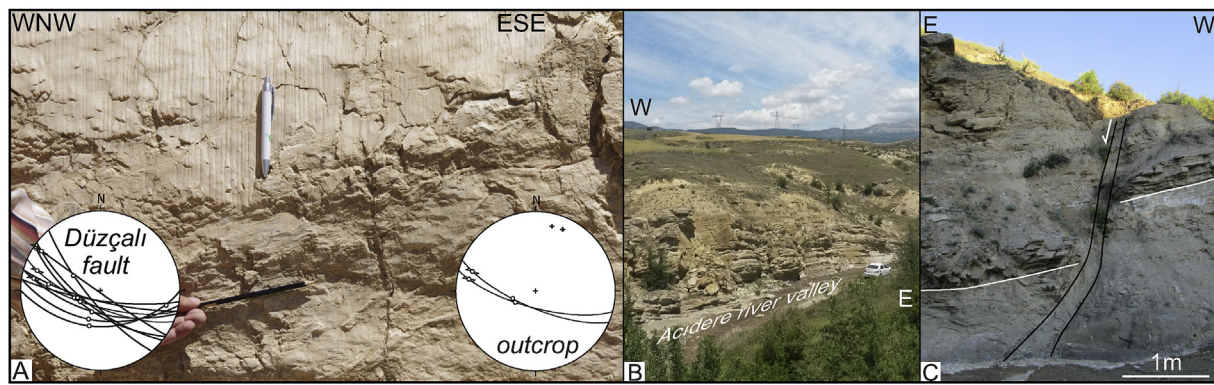
Fig. 3. A) Fault scarp of the western tip of the Düzçalı fault observed in an abandoned quarry in the W-Ballık area. Subhorizontal strike-slip slickenlines (L280/16) overprint steeply-plunging (L285/74) slickenlines. The right stereoplot displays fault and slickenline orientation. The left stereoplot illustrates all observations (including also data from Koçyiğit, 2005) of the Düzçalı fault in the Ballık area. **B**) W-dipping tilted Oligocene deposits in the Acıdere valley in the footwall of the Acıdere fault, Çökelezdağ Horst. **C**) N-S trending, E-facing normal fault affecting Oligocene sandstone and mudstone in the Acıdere valley.

reported as dip direction/dip (e.g. P270/80) whereas linear features are reported as trend/plunge (e.g. L090/85). Fault/fracture orientation analysis is performed with the Stereo 32 (Röller and Trepmann, 2003) and results are visualised in lower hemisphere, equal-area projection stereoplots in the figures. Raw fault/fracture measurements are available for each quarry in Suppl. Mat. S2.

Quarries in the Ballık area were systematically investigated for the presence of faults. The 2013 Google Earth™ satellite image was used as basemap in all figures as this compares most closely with actual quarry situation during the main 2014 fieldwork. Due to continuously moving excavation fronts of the active quarries, quarry walls on current Google Earth images may no longer be in the same position as indicated in the figures in this study. Accurately-taken GPS points of individual observations (with a Trimble Geoexplorer GPS) were used to analyse if the position of the analysed excavation fronts was different than that on the Google Earth satellite image. GPS points are indicated on the fault map figures as small white dots to illustrate where faults were observed. Between travertine quarries, these individual fault observations were strategically linked to map out along-strike fault continuity.

A paleostress analysis is performed on the fault dataset. Principal stress directions can be derived from inversion of fault slip kinematic data. Most paleostress inversion techniques assume the Wallace-Bott hypothesis (Wallace, 1951; Bott, 1959), which state that fault slip should occur parallel to the resolved shear stress on a pre-existing or newly formed fault plane. Inversion of fault-slip data involves the concept of deriving a best-fitting tensor that can explain the direction of slip of the observed faults. The paleostress tensor and the principal stress directions responsible for the (re)activation of the observed faults were derived from the Right Dihedral Method (Angelier and Mechler, 1977) optimised in the Win-Tensor Program (version 5.0.2). This program has the advantage that based on their kinematic features, different phases of faulting can be separated semi-automatically. The different applied steps and quality control of paleostress inversion are described in Delvaux and Sperner (2003) and in Kipata et al. (2013).

4. Structural analysis of the Ballık area

To facilitate the description of the structural features, we separate the study area in different domains. This separation is based on the observed fault kinematics characterising each domain. We first focus on 4.1) large-scale faults cutting through the Ballık travertine. If only extensional features are observed in the quarries, we grouped quarries to the *extensional domain* and describe a 4.2) NE and 4.3) NW extensional domain. When strike-slip reactivation features are observed on extensional faults, we grouped the quarries to the *extensional and strike-slip reactivated domain* in which an 4.4) eastern and 4.5) western part are

described. Quarries that only show strike-slip features are grouped to the 4.6) *strike-reactivated domain* which occurs *in the footwall of Düzçalı fault*. Finally, in 4.7) the deformation of the Killik domal area and the Southern Ballık area are described.

All information on domains, fault data, quarry locations, fault observations and dip of the studied travertine masses are provided in a Google Earth™ kml file in Suppl. Mat. S1. Raw fault-fracture orientations are provided for reproducibility as *.csv files in S3. Here below each quarry is shortly described. A full report on the fault characteristics in each quarry and its travertine facies can be found in Suppl. Mat. S4.

4.1. Large-scale faults: the Elmalı, Düzçalı, Killik and Acıdere faults

Several kilometre-scale faults cross-cut the Ballık area and can be deduced from the morphology of the mountain range-front. The WNW-trending Küçükmalıdağ fault zone delimits the NE incipient margin of the DGHS. This two-to three kilometre wide and 10 km long fault zone developed at the base of the Küçükmalı and Malıdağ mountains and consists of three fault sets: i.e. the Düzçalı, the Küçükmalıdağ and Elmalı faults along which Jurassic-Cretaceous dolomitic limestone, Upper Oligocene conglomerate, Middle Miocene clastics and Quaternary travertine and alluvial-plain sediments are tectonically juxtaposed (Koçyiğit, 2005). At the base of the Küçükmalı mountain (east of the cement factory, Fig. 2), eroded Neogene terraces dip towards the mountain flank due to activity along the listric Elmalı fault.

The Düzçalı fault consists of four SW-, graben-facing, left-stepping fault segments of ~1 km in length. These segments can be traced in the field as the footwall is always a steep hill that consists of travertine, whereas the hangingwall has a gentle topographic slope along which fan-apron cover sediments are deposited. According to Altunel (1994) and Koçyiğit (2005), normal displacements along the Düzçalı fault reach up to c. 200 m. Fault surfaces dominantly contain steeply-dipping slickensides with only a minor dextral strike-slip component. However, in a small abandoned quarry at the western end of the Düzçalı fault subhorizontal strike-slip slickenlines (L280/16) overprint older steeply-plunging dip-slip slickenlines (L285/74) on a fault scarp (Fig. 3A, Fig. 12) and indicate fault reactivation. This observation explains why both normal and strike-slip slickenlines were reported in the Düzçalı fault orientation analysis of Koçyiğit (2005).

The Killik fault, which defines the southern border of the Killik dome, has a dominant WNW-ESE orientation (Fig. 2). In the east, its orientation changes from WNW-trending to NE- and ENE-trending as a left-lateral step-over towards the Elmalı fault. In the west, south of the Tetik and Özçınar quarries (Fig. 2), fault orientation remains NW-SE but its position is displaced by 500 m southwards as can be seen by the

change in morphology of the mountain range-front. The Killik and El-malı faults are considered to be active as indicated by range-front hy-drothermal springs and few small-magnitude earthquakes, such as for instance the 3 November 1993 M_L 3.6 and 12 April 1994 M_L 3.3 earthquakes (USGS Earthquake Catalog, 2018).

West of the Ballık area, the DGHS is bordered by the N-S oriented, steeply E-dipping Acıdere normal fault (Figs. 1 and 2). This fault has a topographic expression because Quaternary sediments in the hanging-wall form the flat basin floor of the DGHS, whereas the hills and older Neogene deposits in the footwall are strongly eroded due to the uplift of the Çökelezdağ Horst (Figs. 1 and 2). The footwall of the Acıdere fault is eroded by the Acıdere river (Fig. 3B). In the Acıdere valley alternating Oligocene sandstone and mudstone beds are exposed of which bedding alternates between NW- and W-dipping and is gently folded (see bed-ding in NW corner of Fig. 2). The fact that these Oligocene beds tilt to the west is related to backtilting of the Çökelezdağ Horst. Few N-S-trending, E-facing normal faults (Fig. 3C), i.e. parallel to the Acıdere fault, affect these sediments and demonstrate the N-S faulted nature of this horst structure.

4.2. NE extensional domain: Kömürcüoğlu, Pamukkale & Gama quarries

In the north-easternmost part of the Ballık area, the **Kömürcüoğlu** travertine is excavated (Figs. 2 and 4). Based on bedding orientation of travertine and the abundant presence of thin paleosols and intercalating conglomeratic layers, a WNW-ESE-oriented mound travertine structure is recognised. In the northern part of the quarry, travertine dips gently (< 10°) to the NNE. The cross-section morphology of the mound ex-hibits a lobe geometry. The central part of the lobe is characterised by a sub-horizontal facies. Towards the southern part of the quarry, this subhorizontal facies changes to a smooth slope facies and biohermal reed facies and dips gently to steeply (> 30°) to the SSW (Fig. 4B-B′). The top of the mound structure is covered by clastic sediments in-cluding conglomerates, sandstone and marls. These sediments thicken from the NW to the SE suggesting a WNW-oriented dip of the top of the mound travertine structure (Fig. 4A-A′). In the southern part of the quarry, a 10 m-thick clastic layer of alternating layers of marls and sandstone laterally interfingers with the SSW-dipping end of the tra-vertine structure (Fig. 5A). These layers are covered by subhorizontal travertine.

The majority of normal faults crossing the Kömürcüoğlu travertine have a NW-SE orientation. In the southern part of the quarry faults are vertical to mostly steeply (up to 50°) north-dipping and have a dip-slip northward normal displacement (Fig. 5B and C). In the northern part, all faults are subvertical to steeply south-dipping and have a decimetre-to metre-scale southward normal displacement (Fig. 5G). The location where faults change from N- to S-dipping lies close to the centre of the travertine mound structure. Slickenlines on the fault walls are always dip-slip, only slightly deviating from verticality (Fig. 5D).

Faults crossing the cover sediments (illustrated separately in Fig. 4) are not used for paleostress inversion. Each fault has its own complex formation history. Opposite fault walls are often symmetrical (Fig. 5C) and are typically characterised by multiple succeeding phases of faulting, fault-parallel fluid flow, dissolution, brecciation and devel-opments of striations by mechanical friction (Fig. 5D and E). Each of these different phases can later be cemented due to secondary fluid circulation. The faults are filled by brown oxidised mud, travertine clasts, debris and organic-rich material. The muddy and chaotic infill is indicative of the open nature of the faults during extension, enlarged by dissolution of the fault walls. Slickenlines are not always visible on the fault plane as secondary fluid flow has often overgrown these kinematic markers.

Joints orientations are similar to those of the faults. In the northern part of the quarry, joints are vertical and are NW-SE-to E-W oriented whereas in the southern part, the joints are steeply north-dipping and have a NW-SE to WNW-ESE orientation. Also a minor population of NE-

SW- to NNE-SSW joints has been observed.

In a small quarry south of Kömürcüoğlu (S. quarry in Fig. 4), metre-scale caves emplaced in biohermal reed facies are present (Fig. 5F). At the top of the cave hanging, pillar-shaped bryophytes are coated by cements giving rise to stalactite-like appearances hanging from the cave ceiling.

The **Pamukkale** and **Gama** quarries (north of the cement factory, Fig. 3) excavate a WNW-ESE trending domal structure with NNE- and SSW-dipping flanks (Fig. 6A-A′). Faults are absent in the Gama quarry. In Pamukkale, small, decimetre-scale displacement normal faults cut the abundant thin paleosols. Faults are vertical to steeply N- and S-dipping and have a NW-SE trending orientation, which slightly deviates from the two large SW-oriented normal faults that limit the southern edge of the Pamukkale travertine. The travertine in the hangingwall of these faults is tilted with bedding steeply SW-dipping (~45°) (Fig. 6A-A′, D). Gravity-driven, fan-apron slope deposits, including unsorted, irregularly-oriented travertine blocks set in a sandy to marly matrix, cover the hanging walls of these normal faults (Fig. 6B–D). Fault history is characterised by numerous different stages of fracturing, fluid flow, brecciation and mechanical friction creating slickenlines (Fig. 6E). Joint population can be subdivided in three distinct, mutual abutting joint sets which are oriented WNW-ESE (parallel to the observed faults), NNE-SSW and E-W.

4.3. NW extensional domain: Kepez and Taşkestik Tepe

At the highest point of the northern graben edge, the **Kepez Tepe** and **Taşkestik Tepe**, two individual travertine domal bodies, are ex-posed (Fig. 7). In the NW, a WNW-ESE oriented travertine body is ex-cavated in a presently abandoned quarry (Ab$_1$). Travertine dips gently to the NNE and is cut by WNW-ESE oriented normal faults (Fig. 7C-C′). Displacement is mostly to the SSW. At the southern end of the tra-vertine mass in Ab$_1$, bedding is dipping moderately to SSW due to block rotation along a listric normal fault (Fig. 7C-C′).

A metre-thick gravel layer is present in the travertine. Joints are limited to the travertine and do not continue into the gravel. The thick muddy infill of these joints (Fig. 7D and E) suggests that joints are dissolution enlarged by weathering of the fracture walls.

The travertine dome on the **Taşkestik Tepe** (Ab$_2$) is also WNW-ESE oriented. Travertine dominantly dips to the NNE due to block rotation. At its lateral end, gently SSW-dipping layers are exposed (Fig. 7F, H-H′). These SSW-facing normal faults affect the dome and can have dis-placements up to 10 m. These normal faults are consistent in orientation and can be traced for several hundred metres through the different quarries on the Taşkestik Tepe. Joint orientation is dominantly parallel to the faults.

4.4. Eastern extensional and strike-slip reactivated domain: Karakurt, Stone Terroir, Reisoğlu, and Özaş quarries

In the Karakurt, Özhan and Stone Terroir quarries a continuous NW-SE oriented, subhorizontal travertine mass is excavated. Subvertical NW-SE to NNW-SSE normal faults with decimetre-to metre-scale, al-ternating NE and SW displacement cut the travertine body in **Karakurt**. The NE part of Karakurt is cut by a south-dipping, left-lateral strike-slip fault. The SW edge of Karakurt is cut by a SW-dipping normal fault (Fig. 8B) that can be connected to a 5 m-wide, open fault zone in the centre of Stone Terroir (Fig. 8C-C′).

In **Stone Terroir**, bedding changes from subhorizontal (lateral equivalent of Karakurt) to gently SW-dipping (~15°), forming the SW edge of the Karakurt-Özhan-Stone Terroir travertine mass. Slickenlines on the fault infill are indicative of strike-slip reactivation. The SW edge of the travertine body is cut by a SW-dipping normal fault (Fig. 8C-C′, D). The Stone Terroir travertine is covered by muds, marls and rotated travertine blocks (Fig. 8D).

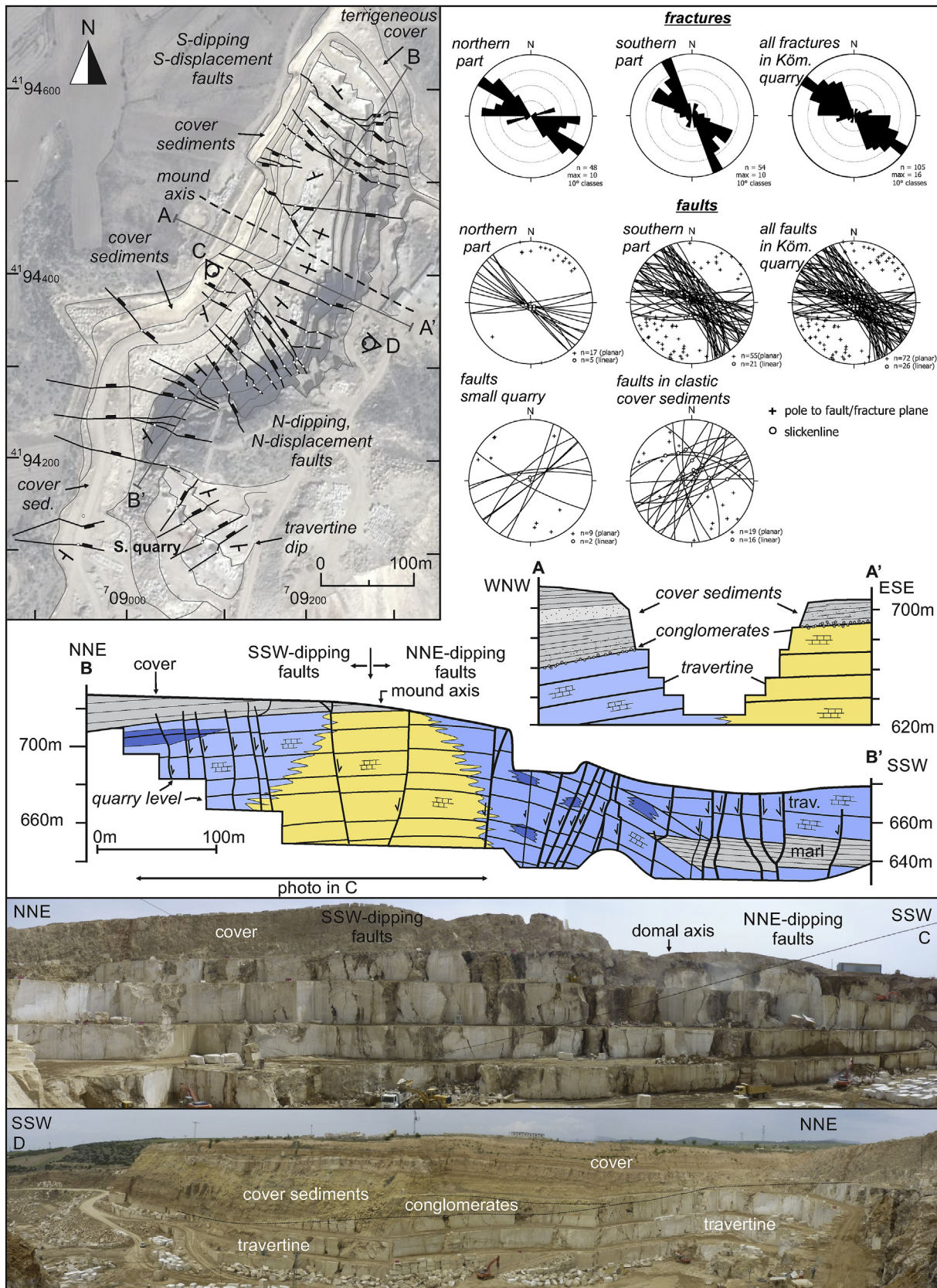In the upper levels of **Reisoğlu**, a domal axis is visible with bedding

Fig. 4. Fault map (basemap © Google Earth) and fault/fracture kinematic analysis (stereoplots) of the Kömürcuoğlu travertine (NE Ballık area). Note the different orientation of the faults in the small quarry in the south (S. quarry). The combined sedimentological and structural model shows that central sub-horizontal travertines (yellow) laterally continue into sloping cascade (blue) and waterfall facies (dark blue). The northern part is cut by upright to steeply S-dipping fractures and normal faults, with a southwards displacement, whereas the southern part is cut by north-dipping faults with northwards displacement. NW-dipping marly, conglomerate and sandstone (A-A′) cover the travertine dome. Marly deposits interfinger with the travertine structure (southern part of B-B′). (For interpretation of the references to colour in this figure legend, the reader is referred to the Web version of this article.)
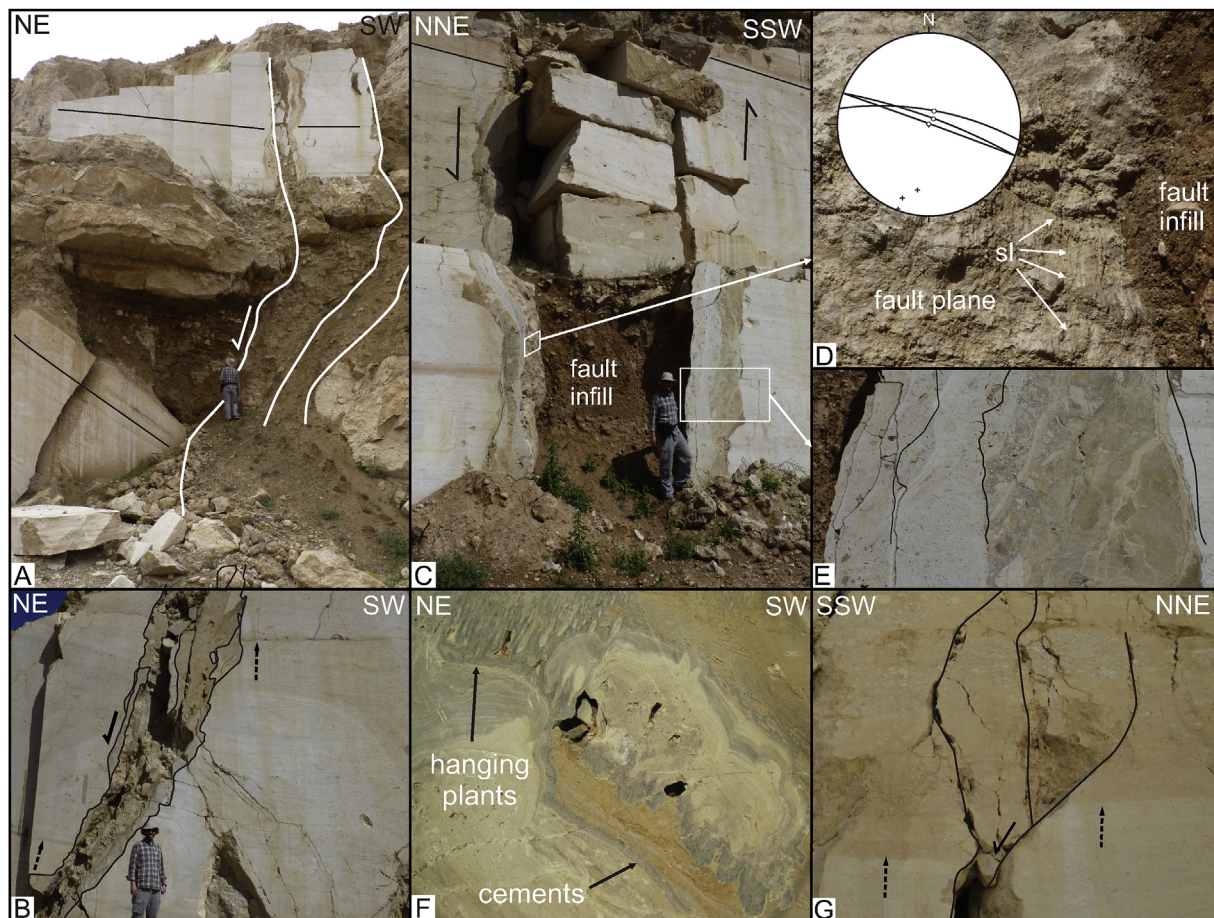
Fig. 5. Kinematic features observed along of the Kömürcuoğlu faults. **A)** Interfingering marls and sandstone layers in the southern part of the quarry. Note the fault orientation change when it crosses the clastic sediments and travertine contact. **B)** Northwards displacement of a normal fault in the S part of the quarry. **C & E)** Open normal fault in the S part of the quarry. Fault walls characterised by a complex build-up indicative of multiple phases of faulting, lateral fluid flow and brecciation. Fault filled by mud and travertine blocks. **D)** Dip-slip slickenlines (sl) observed in the hangingwall of the fault in c). **F)** Stalactite-like features hanging from a cave ceiling. Cavity infill by cement precipitation of hanging plants observed in the small quarry (S. quarry). Cement infill around the cave. **G)** Contact between travertine and conglomeratic cover. Southwards displacement of a N-dipping normal fault in the northern part of the quarry.

oppositely NNE- and SSW-dipping (Fig. 8A-A′). This travertine body can laterally be followed towards **Özaş** where only the NE-dipping flank is excavated. A long SW-dipping normal fault with c. 20 m SSE displacement is present in the centre of Özaş (Fig. 8E, F-F′). The travertine in the centre of the Özaş quarry is collapsed due to extension (Fig. 8G).

4.5. Western extensional and strike-slip reactivated domain: Aydın, Sorkun, Simersan, Tuna and Emek quarries

The Sirmersan, Sorkun, Upper Tuna, Aydin, Sorkun Ab., Faber Ab. quarries excavate a continuous NW-SE oriented 1.5-km long travertine geobody.

Aydın is characterised by three, meters-wide, WNW-ESE-oriented bifurcating fault zones (Fig. 9B and C) filled with mud and travertine blocks. Slickenlines range from subhorizontal with a NW-SE trend, to gently SE- and NW-plunging, indicative of left-lateral strike-slip and oblique-slip faulting. A 600 m long fault zone can be traced from the upper part of Aydın to the SE end of Sorkun Ab. The NW end of this strike-slip fault zone can be traced through the landscape as its prolongation forms the transition between the flat field NE of Sorkun and the steep flank at the foot of the Taşkestik Tepe.

Most normal faults in the upper Ballık area are SW-facing towards the graben floor. Between Aydın and **Upper Tuna**, however, two steeply, NE-dipping normal faults occur (Fig. 9D). Bedding was tilted to a steep SW-dipping attitude (P207/50) due to small-scale block rotation

along these faults. NNE-SSW to NE-SW and NW-SE oriented joint sets are congruent to the two fault populations in Upper Tuna.

In **Sorkun**, left-lateral strike-slip faults with brecciated fault cores developed. Joint orientation is very irregular. The regional NW-SE joint set is still present, but also other moderately dipping joint sets cut the travertine.

In **Sirmersan**, two small travertine bodies are excavated. These bodies are covered by a marly sedimentary unit that continues northwards to the base of the Kepez Tepe. The travertine is cut by rare strike-slip faults and by one N-facing normal fault with a thick fault infill. NW-SE and E-W joints are the most abundant.

In the **Emek** quarry and in its abandoned part (**Emek Ab.**), travertine dips gently to the NNE and consists mainly of a flat-pool facies. Faults and joints are consistently parallel and have a steeply SW-dipping attitude (see stereoplots in Fig. 9). The northern part of Emek travertine is cut by three strike-slip faults (Fig. 9G). The northernmost fault forms the NE excavation front of the quarry and is filled with a coloured mud rich in iron (brown) and manganese (black) oxi/hydroxides (Fig. 9H). Gently (L100/20) to moderately ESE-plunging (L130/40) slickenlines, indicative of strike- and oblique-slip, respectively, overprint steeply-plunging striae (L230/80). Paleosol displacements along SW-dipping fault planes (P210/80) containing NW-plunging slickenlines (L302/05) indicate left-lateral strike-slip.

In the central part of the active Emek quarry, several parallel, closely-spaced (20 m spacing) normal faults, with the largest one
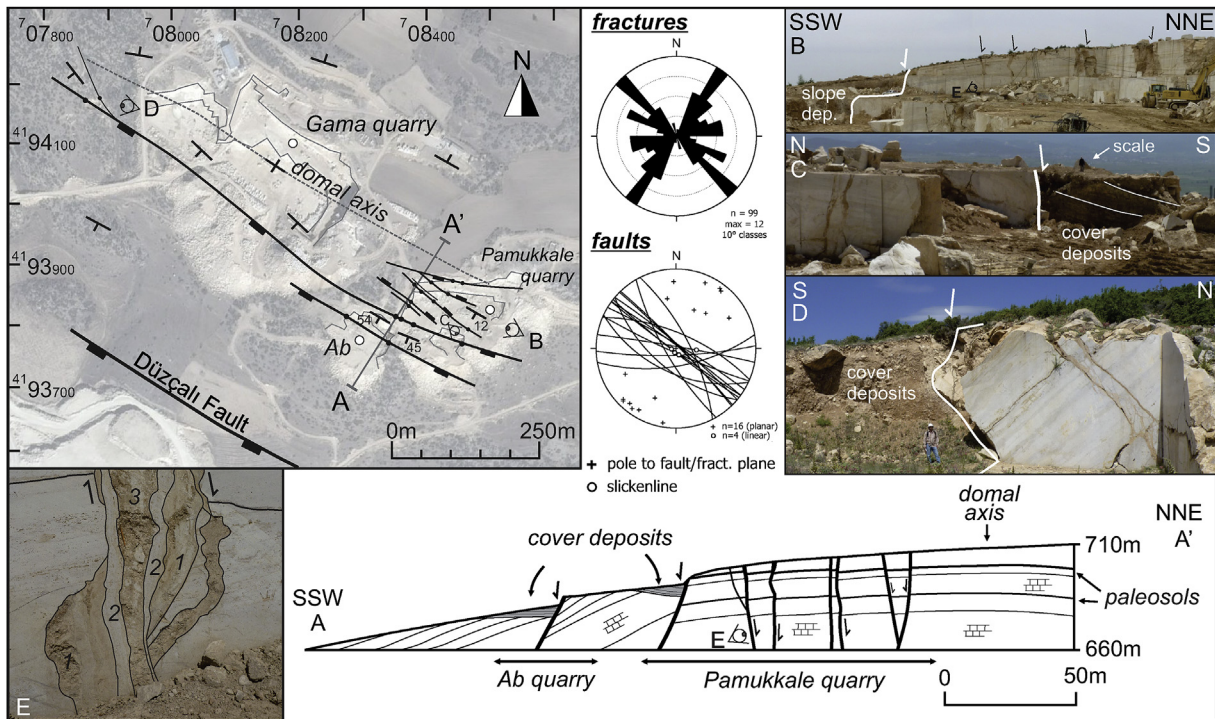
Fig. 6. Fault map (basemap © Google Earth) and kinematic analysis (stereoplots) of normal faults observed in the Pamukkale and Gama quarries (NE Ballık area). **A-A′)** Travertine is cut by normal faults. **B)** Overview of the Pamukkale quarry and minor normal faults. **C-D)** Two normal faults cut the southern edge of the Pamukkale-Gama travertine dome. Note the abrupt change of travertine into slope deposits or marls. **E)** Complex fault with several deformation and infill phases.
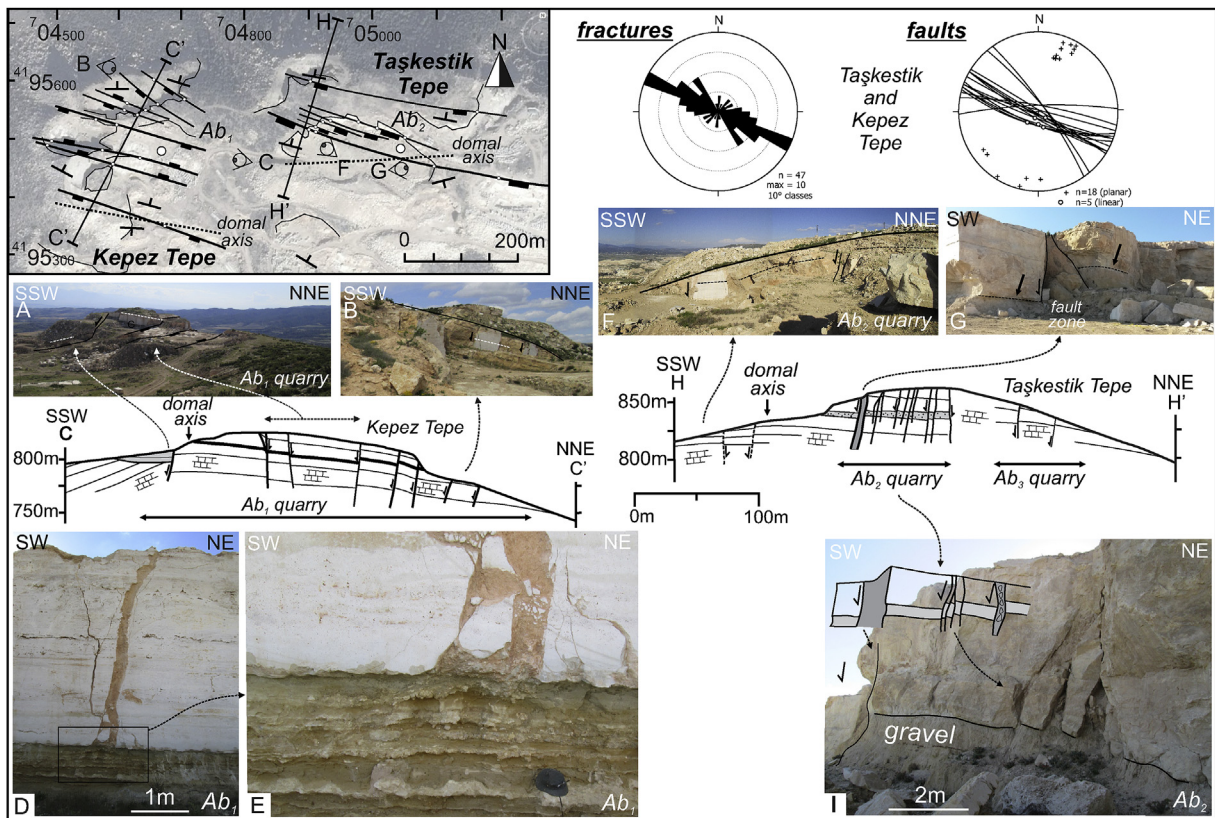

Fig. 7. Fault map (basemap © Google Earth) and fault/fracture kinematic analysis (stereoplots) of the Abandoned quarries on Kepez Tepe and Taşkestik Tepe. **C-C′)** Normal faulting through the travertine on Kepez Tepe. Note the change in bedding orientation due to activity along the SSW-most normal fault (**A**) and the NNE-dipping bedding in Ab$_1$ (**B**). **D-E)** Dissolution-enlarged and clay-filled fracture cutting the travertine but arresting on the gravel-travertine contact. **H-H′)** Graben-facing normal faulting affecting the travertine on Taşkestik Tepe. **I)** Subparallel faults displacing a thick travertine-intercalating gravel layer.
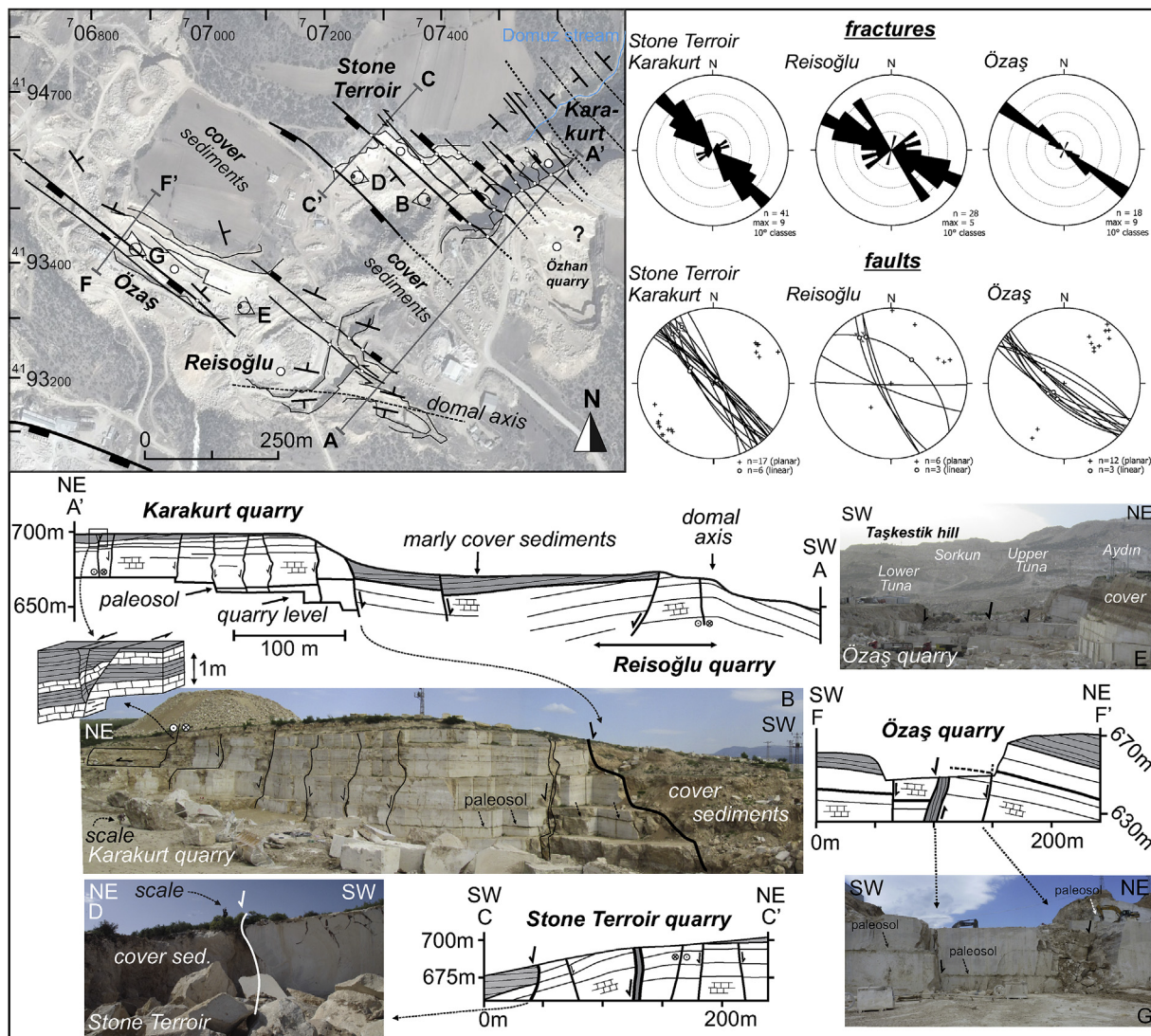
Fig. 8. Fault map (basemap © Google Earth) and fault/fracture kinematic analysis (stereoplots) of Karakurt, Stone Terroir, Reisoğlu and Özaş quarries. **A-A′)** Cross-section through Karakurt (**B**) and Reisoğlu quarries. In the NE part of Karakurt, a sinistral (transtensional) strike-slip fault with horizontal striae is present. **C-C′)** Structure of Stone Terroir quarry. Large normal fault at the SW edge. **D)** Slope deposits covering the hangingwall. **E)** Marly-sandstone sequence covering the Karakurt-Stone Terroir and the Özaş-Reisoğlu travertine bodies. **F-F′)** A wide SW-dipping normal fault zone with more than 20 m displacement cuts the NNE-dipping Özaş travertine mass. A 0.5 m-thick paleosol (**G**) and the marly-sandstone cover are displaced over 20 m by this fault.

displacing an up to 20 m displacement, are present (Fig. 9F-F′, G). Similarly to observations in other quarries, faults had an open nature in which circulating fluids precipitated as carbonate cements along fault planes (Fig. 9K).

Emek Ab. is bordered in the SSW by a hectometre-long fault zone. Travertine bedding in the footwall is gently NNE-dipping. The hangingwall is composed of coarse-grained sandstone layers with a steeply SSW-dipping attitude (P232/62) (Fig. 9J). This sandstone is situated on a higher stratigraphical and structural position than the Emek travertine body and represents an interfingering clastic facies.

The 20 m-displacement, normal fault zone crossing the Emek travertine continues towards the **Lower Tuna** quarry. Here, travertine dips gently to the NNE and marl and mud deposits cover the hangingwall of this wide fault zone (Fig. 9A-A′, E). The northern NE-dipping fault wall (P040/81) is marked by WNW-plunging slickenlines (L300/48), indicative of normal faulting with a substantial oblique-slip component.

4.6. Strike-reactivated domain in the footwall of Düzçalı fault: best, Cinkaya, Faber W, Tetik and Özçınar quarries

In the **Best** quarry and in two adjacent abandoned quarries (Ab₁ and Ab₂ in Fig. 10), numerous parallel, closely-spaced, NW-SE to WNW-ESE-trending strike-slip faults (Fig. 10A, B-B′) cut the travertine. The often metre-thick sedimentary fault infills consist of brown, chaotically-ordered oxidised muds, small travertine blocks and organic-rich material (Fig. 10C–E). Successions of paper-thin, brittle, calcite rafts are present in the fault, indicating that during fault development circulating fluids stagnated for a certain period in the open fault (cf. El Desouky et al., 2015, Fig. 10D). Fault planes are coated by white to brown calcite cements giving them a nodular-shaped appearance. Slickenlines and slickensides are mostly only present on the polished cemented nodule-shaped surfaces and on the muddy fault infill, but never as mechanical striations on the travertine rock itself (Fig. 10F). Mineral steps on the slickensides all indicate left-lateral shear suggesting that strike-slip faulting occurred after fluid flow along the fault planes.

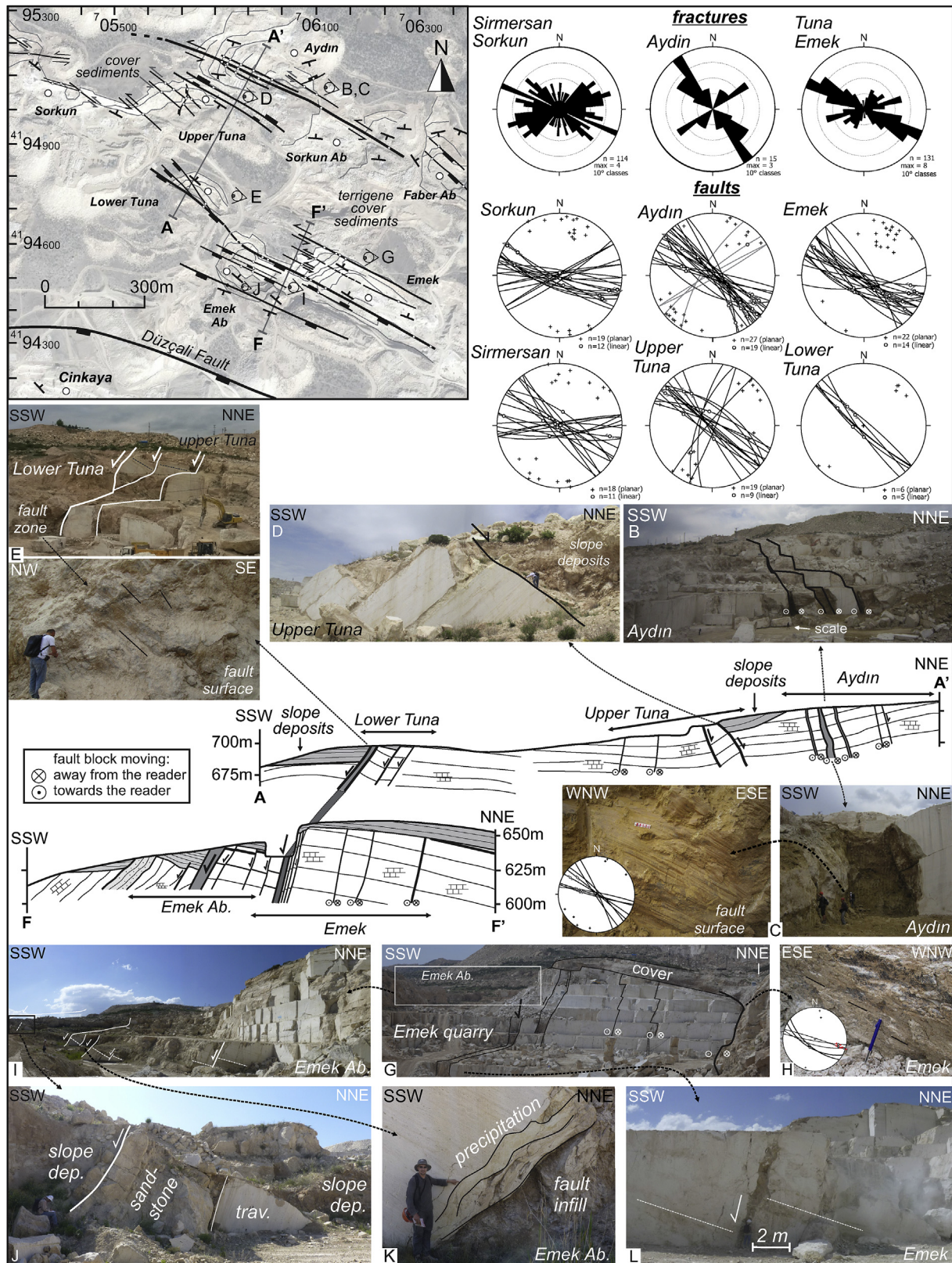Joint sets show a large variety in orientation. Joints are parallel to

Fig. 9. Fault map (basemap © Google Earth) and kinematic analysis (stereoplots) of faults in the Emek, Lower and Upper Tuna, Aydın, Sorkun and Sirmersan quarries (NW Ballık area). **B & C)** Metre-wide, open strike slip fault zones with gently plunging slickenlines in Aydın. **D)** Block rotation in Upper Tuna. **E)** SW edge of the Tuna travertine mass which is bordered by a m-wide normal fault. **F-F′)** Emek cross-section. **G)** Closely-spaced strike-slip faults in Emek. **H)** Overprinting strike-slip striae on fault infill. **I)** Normal faulting in Emek Ab. **J)** SW- edge of Emek Ab. where sandstone layers cover the Emek travertine mass. **K)** Precipitation along fault planes. **L)** Normal faulting in Emek.
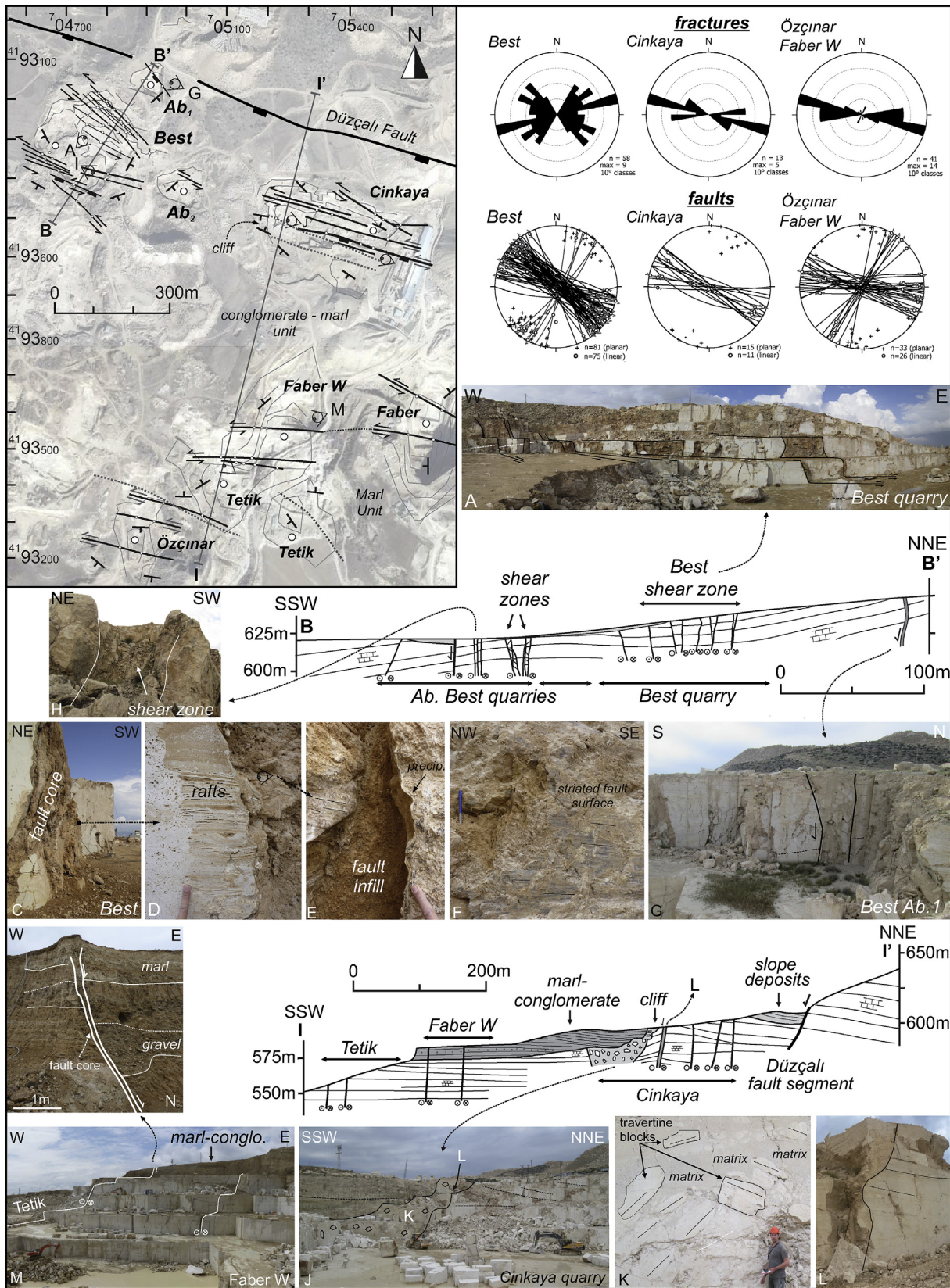
Fig. 10. Fault map (basemap © Google Earth) and fault/fracture kinematic analysis (stereoplots) of the Cinkaya, Best, Faber W, Tetik and Özçinar quarries (NW lower Ballık area). **A)** NW-SE to WNW-ESE strike-slip faults in Best. **B-B′)** Cross-section through the shear zone in Best. **C)** Fault core. **D-F)** Disrupted muddy fault infill, successions of thin, brittle rafts and cementation/precipitation along the fault wall. Striated polished nodular-shaped fault wall in E. **G-H)** Open faults with infill of travertine blocks. **I-I′)** Düzçalı fault to Tetik quarry cross-section showing NNE-dipping travertine in Cinkaya and subhorizontal facies in Faber W and Tetik. **J)** The marl-conglomerate layer (also discussed in Claes et al., 2015) starts from a cliff (**L**) and covers the travertine of Faber W and Tetik. **K)** Travertine blocks floating in a muddy matrix. **M-N)** Strike-slip faults in Tetik and Faber W. continue through the marl-conglomerate layer cover.

the WNW-ESE faults, but also an apparent dominant ENE-WSW joint set is present in the Best quarry. Considering the small angle (~50°–70°) between both joint sets, they could reflect conjugate jointing that formed during shear deformation.

In **Cinkaya**, bedding is subhorizontal in the middle part, NNE-dipping in the northern part and SSW-dipping in the SW part of the quarry. Along the western quarry flank, the SE-dipping travertine mass is abruptly cut by a steep, stepwise erosional cliff (Fig. 10I-I′, J, L). A debris layer covers the travertine along the southern edge of this cliff. In this debris layer, large travertine blocks are irregularly piled up and are 'floating' in a fine-grained travertine matrix (Fig. 10K). The debris layer can be laterally traced through Cinkaya in a WNW-ESE direction. Similar cliff-like structures are described along the Honaz fault zone where they are exposed as fault scarps along major fault segments (Koçyiğit, 2005). These similarities suggest that the cliff in Cinkaya represents an ancient, synsedimentary inactive fault.

WNW-ESE, left-lateral strike-slip faults can be followed from Best to Cinkaya. On a normal fault in the centre of Cinkaya, steeply-plunging slickensides are overprinted by subhorizontal slickenlines indicating that the normal faults are strike-slip reactivated. Joints are consistently parallel to the mapped faults.

The marl-conglomerate alluvial plain unit, of which the debris layer forms the base, continues to the south, where it reaches a thickness of 20 m. It covers the **Faber W** travertine mass (Fig. 10M) and thins out to the east in the Faber quarry (i.e. referred to as the marl-conglomerate occurrence in Claes et al., 2015).

Faults in **Faber W**, **Tetik** and **Özçınar** are dominant WNW-ESE oriented with subhorizontal E-to W-plunging subhorizontal slickenlines and sometimes clear left-lateral slickensides (Fig. 10). In the sedimentary marl-conglomerate cover, a normal, northwards-oriented displacement of 2 m has been observed (Fig. 10N). Evidence of post-sedimentary faulting are clay smearing of the incompetent marly layers inside the fault zone and thickening of a conglomerate layer at the intersection of the fault and the antithetic fault. Clast rotation (cf. Loveless et al., 2011) cannot be observed due to the fact that clasts are spherical. Inside the travertine mass, subhorizontal left-lateral strike-slip kinematics are found along the fault wall of the same fault, indicative of fault reactivation.

4.7. Killik domal area and Southern Ballık area

Tectonic deformation and development of the fault/fracture network affecting the Killik domal area (Faber, Ece, Tetik, Çakmak, İlik, Alimoğlu and Best Ab. Quarries, see Fig. 2) have been extensively studied by Van Noten et al. (2013). The Killik dome continues towards the east where it is excavated within the Alimoğlu Tasarim, Demmer, Başaranlar, Metamar and Şiray quarries.

Along the northern flank of the Killik dome (**Alimoğlu Tasarim, Metamar**) travertine is mostly subhorizontal and is covered by a thick marl-conglomerate facies. Alimoğlu Tasarim is dominated by joints that bifurcate in the cover sediments. In Metamar (Fig. 11), NW-SE normal faults are parallel to the Düzçalı fault and have NE- and SW displacements.

The travertine in the SW part of the Killik dome (Çakmak, İlik, Alimoğlu and Best Ab) changes from horizontally bedded at the base towards a more complex low-angle slope facies near the upper part. The eastern domal part (**Demmer, Başaranlar** and **Şiray**), however, consists of subhorizontal bedded travertine dipping gently to the SSW and SSE. The fact that the complexity of the Killik dome does not continue towards the east, suggests that either other major sources may have been present to cause the formation of the travertine in Demmer and Başaranlar or that these travertines formed in a later timing and different flow path but from the same spring location. E-W oriented normal faults cut the edge of the travertine in Başaranlar. In Şiray, faults are E-W oriented and show evidence of both normal and strike-slip faulting.

Few abandoned quarries (**Faber Ab.**) are present in the area below the cement factory and north of the Killik fault. Here, a small, NW-SE oriented domal structure, with opposite NE- and SW-dipping flanks is present. Based on the orientation of this structure and the absence of any connection with the Killik dome, a different source can be assumed. This travertine mass is cut by several NW-SE oriented normal faults with subhorizontal slickenlines on the fault infill.

Contrary to the tilted blocks along the northern flank of the DGHS, the Killik dome is not affected by block tilting. Faults have a different orientation along both flanks of the Killik dome. Whereas NW-SE oriented faults cut the northern flank, E-W to WNW-ESE faults affect the southern part. Based on fault distribution, the rigidity of Killik dome thus seems to have played a role in such way that faults preferentially developed along its flanks after travertine formation but hardly in its centre.

In the Killik dome, fracture propagation is influenced by different travertine facies. Joints that developed in subhorizontal travertine facies are continuous and straight, whereas joints in slope facies have an irregular trace and are affected by the local travertine bedding forming staircase fractures (cf. Maggi et al., 2015). In the northern flank of the Killik dome, i.e. in the NNE-dipping and subhorizontal flanks, joints are dominant WNW-ESE oriented and are parallel to the mapped normal and strike-slip faults affecting this part (Fig. 11). As the northern part is situated in the hangingwall of the Düzçalı fault, joints and faults show a large parallelism to the trace of this fault. In the eastern part of the Killik dome, i.e. in Çakmak, İlik and Alimoğlu, majority of the joints are parallel to the E-W to WNW-ESE oriented faults. Two other significant joint sets, i.e. a NW-SE and a NE-SW oriented set, can be recognised (see also Van Noten et al., 2013). Towards the eastern end of the Killik dome, joints in Başaranlar are NE-SW oriented and deviate slightly from the E-W oriented faults. In Faber Ab., fractures are parallel to the local faults and are dominantly NW-SE trending.

5. Paleostress analysis

Paleostress inversion results in three orthogonal principal stress axes and the stress ratio R = $(\sigma_2 - \sigma_3)/(\sigma_1 - \sigma_3)$, which classifies the stress tensors as radial/pure/strike-slip extensive, extensive/pure/compressive strike-slip or strike-slip/pure/radial compressive stress states. Inversion is sometimes problematic if the observed deformation results from multiphase deformation history and if fault data is heterogeneous (e.g. Çiftçi and Bozkurt, 2009). To overcome this problem, we grouped faults from different quarries that have similar kinematics. To identify different fault populations and stress orientations, we rejected faults with high misfit angles in the Win_tensor Program until a solution with homogeneous faults was found. When a rejected fault population resembled faults in neighbouring quarries, then this population was regrouped into a new subset for which the inversion was rerun. The stress regime index R′ distinguishes between pure extensive, transtension and a pure strike-slip regime (Fig. 12).

Paleostress inversion carried out on the fault data results in two dominant but significantly different stress regimes: NE-SW pure extension (R′ < 0.75) to transtension (0.75 < R′ < 1.25) and a pure strike-slip regime (1.25 < R′ < 1.75) with ENE-WSW compression and NNW-SSE extension. The north-eastern (Kömürcüoğlu, Pamukkale, Gama, Stone Terroir, Karakurt) and north-western (Kepez and Taşkestik Tepe, Sirmersan) areas were only affected by NE-SW extension to transtension (= oblique opening). Travertine at the base of the Taşkestik Tepe was strongly affected by the strike-slip regime.

Locally in the small quarry south of Kömürcüoğlu, the deduced NW-SE extension deviates from regional extension. Because of the local presence of the NE-SW transfer zone between the Düzçalı and the Elmalı faults in this region (Fig. 2), this NW-SE extension might be a local effect and cannot be extrapolated to a regional stress regime.

Travertine in the footwall of the Düzçalı fault and this fault itself bear characteristics of both the NE-SW extension regime (Emek, Özaş,
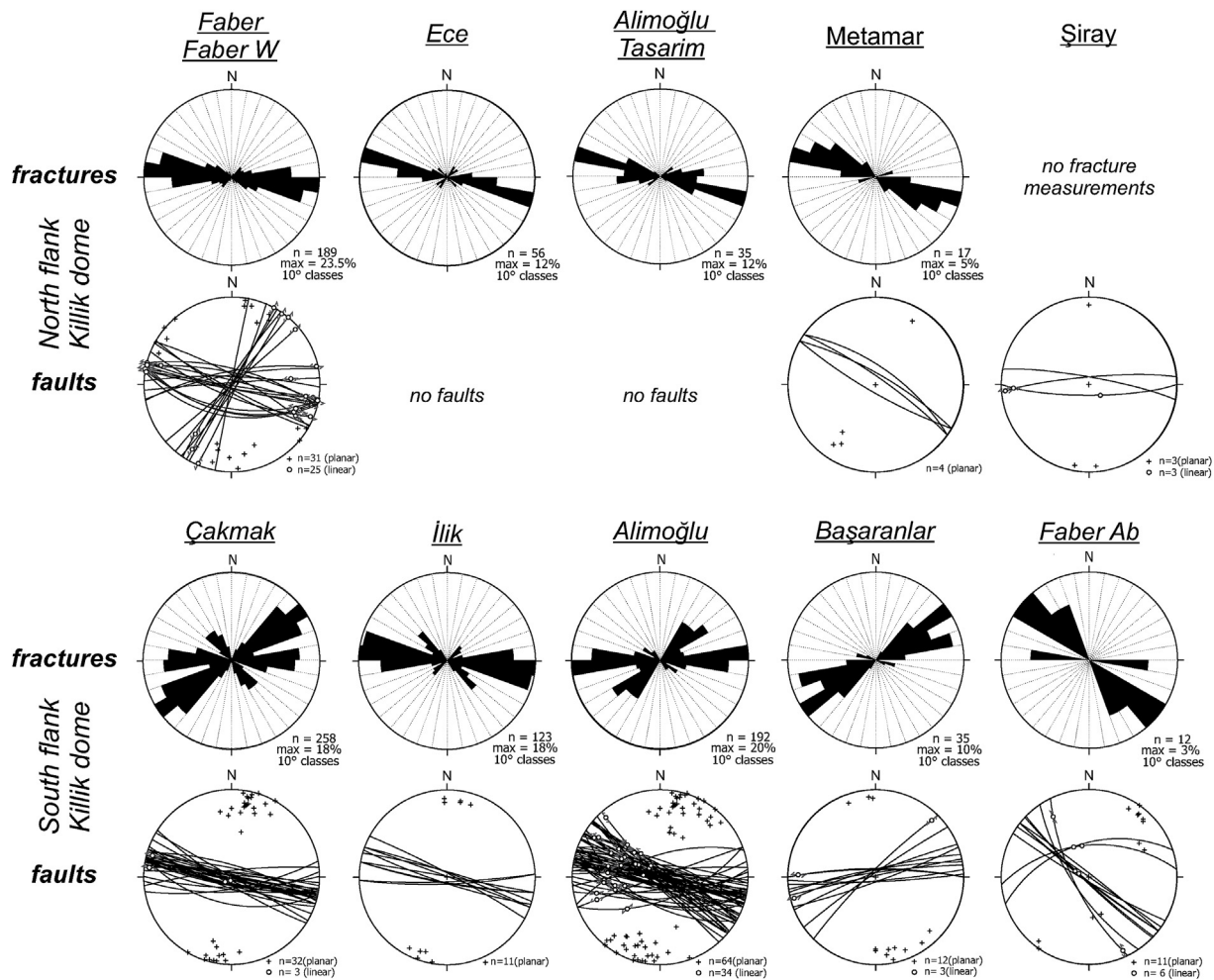
Fig. 11. Fault and fracture orientation analysis (stereoplots) of the Killik dome. See Fig. 2 for quarry locations. Rose diagrams illustrate fracture distribution. Northern and southern flanks of the Killik are separated. Also discussed in Van Noten et al. (2013).

Lower Tuna, Pamukkale, Gama, Düzçalı) and the strike-slip regime (Emek, Emek Ab, Lower Tuna, Düzçalı). Stress inversion of fault data in the lower part of the Ballık area (Tetik, Özçınar, Faber W, Faber, Alimoğlu, Başaranlar) results in the strike-slip regime. Strike-slip kinematics are absent in the middle part of the Killik dome (Metamar, Şiray). Stress inversion shows a slightly different extensional direction with N-S extension.

The NE-SW to NNE-SSW extension that deformed the Ballık area is similar to the current NE-SW to NNE-SSW extension in the eastern and central parts of the DGHS, as indicated by focal mechanisms of recent small to moderate earthquakes (Irmak, 2013) and kinematic analysis of the margin-bounding faults along the Denizli and neighbouring grabens (Çiftçi and Bozkurt, 2009; Kaypak and Gökkaya, 2012).

6. Discussion

6.1. Travertine morphology

Although a detailed travertine facies analysis is beyond the scope of this study, the general dip and morphology of the different studied travertine deposits can be used to identify the morphology of the Denizli margin at the time of Pleistocene Ballık travertine deposition and allows tentatively to locate possible feeder systems. Establishing this morphology is important to separate sedimentological depositional from tectonic deformation processes. In general, in the Ballık area, travertines occur as (large) travertine geobodies deposited in flat pools and in slope-controlled travertine mounds in the eastern part and as

individual travertine domes in the western part.

The Kömürcüoğlu travertine body (Figs. 2 and 3) is oriented E-W, orthogonal to the orientation of the nearby travertines in the Ballık area. Based on depositional geometry of facies, a large fan-shaped mound travertine geobody (Fig. 13) can be proposed, changing upwards from a subhorizontal facies, to a (smooth) slope facies, to eventually the biohermal reed facies. In cross-section (Fig. 13) the mound has a lobe geometry.

In the upper part of the mound, the juxtaposed amalgamation of the biohermal reeds predominate towards the SSW part of the Kömürcüoğlu travertine. These reeds consist of barrages of higher plants, such as bryophytes, reed stems and mosses, that impeded water to flow. Behind these barrages stagnant waters were the cause of the inferred water pool facies. The biohermal reed facies occur along the smooth slopes at both flanks of the mound.

The increasing amount of higher plants (Fig. 5F) towards the top of the deposits represent a cooling and shifting water flow direction and eventually the formation of paleosol intercalations. Several metre-scale primary caves develop below hanging plants. Originally, the formation of these hanging plants should be driven by gravity and should have grown nearly vertically in biohermal reed facies. In the southern part of the Kömürcüoğlu quarry, however, these plant structures have a steep dip of ~70° (Fig. 5F). This observation indicates that this part of the travertine mass was rotated towards the SE by block rotation due to local faulting. Ceasing of travertine deposition is demonstrated by alternation of finer mud sediments and less well-sorted matrix-supported conglomerates that cover the Kömürcüoğlu travertine. The detritals are
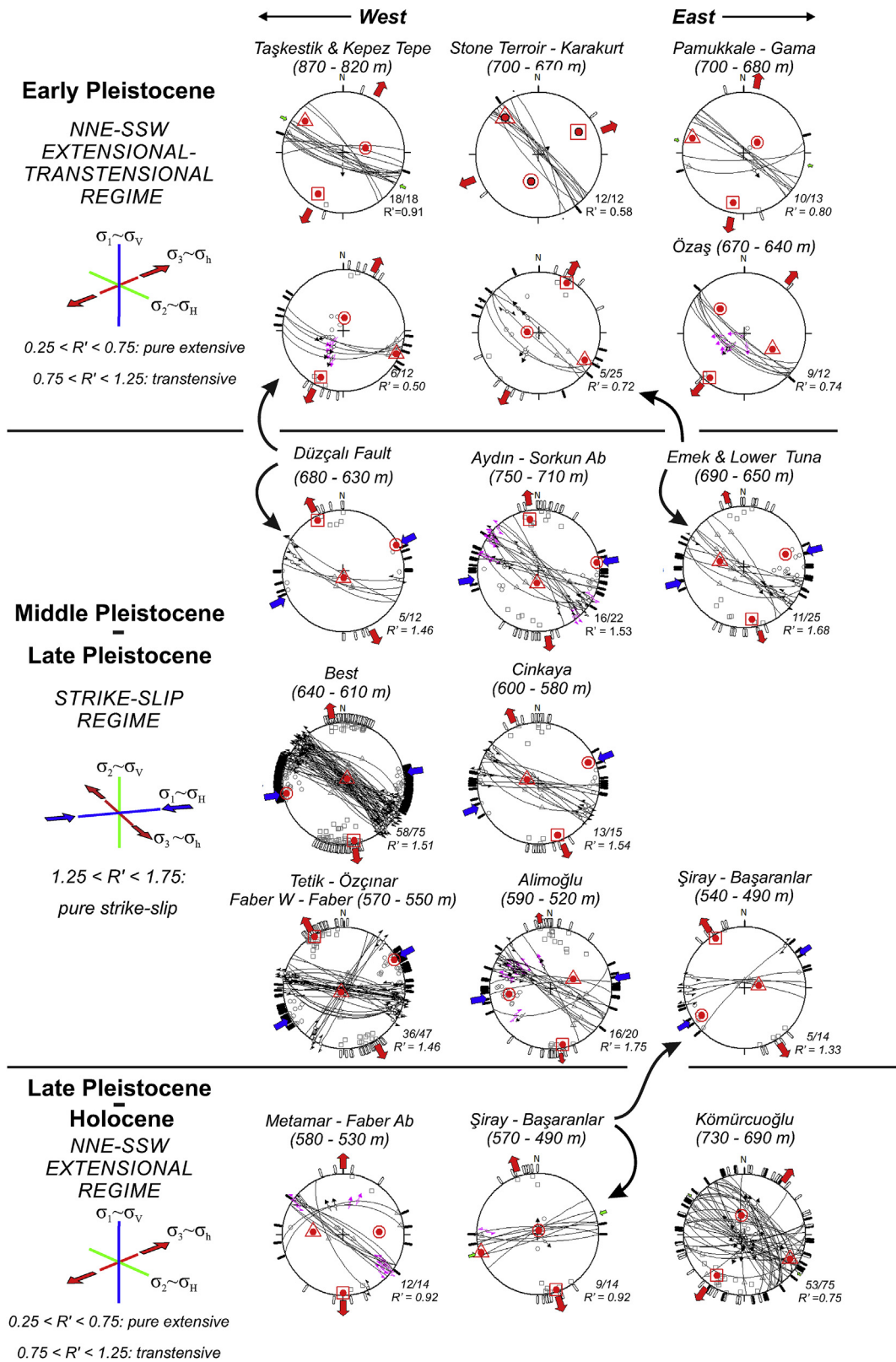
Fig. 12. Win_tensor Program stress inversion results of selected fault data and associated slip planes observed in the Ballık area. Results are subdivided in three stress regimes. On each separate line, quarries are ordered from west to east. Quarry elevation is indicated. Along Düzçalı fault and in Emek, Lower Tuna, Şiray and Başaranlar two stress regimes (see black arrows) are deduced. Düzçalı Fault inversion results from fault data gathered from this study and Koçyiğit (2005). Three principal stress axes: circle for σ_1; triangle for σ_2; square for σ_3. Number of used fault-slip data with respect to the total amount of data for the considered fault data is indicated. R' = stress regime index. Outward arrows indicate extensional deviatoric stresses; inward arrows represent compressional deviatoric stresses. Blue arrows: σ_1 (S_{Hmax}). Green arrows: σ_2 (S_{intm}). Red arrows: σ_3 (S_{hmin}). (For interpretation of the references to colour in this figure legend, the reader is referred to the Web version of this article.)
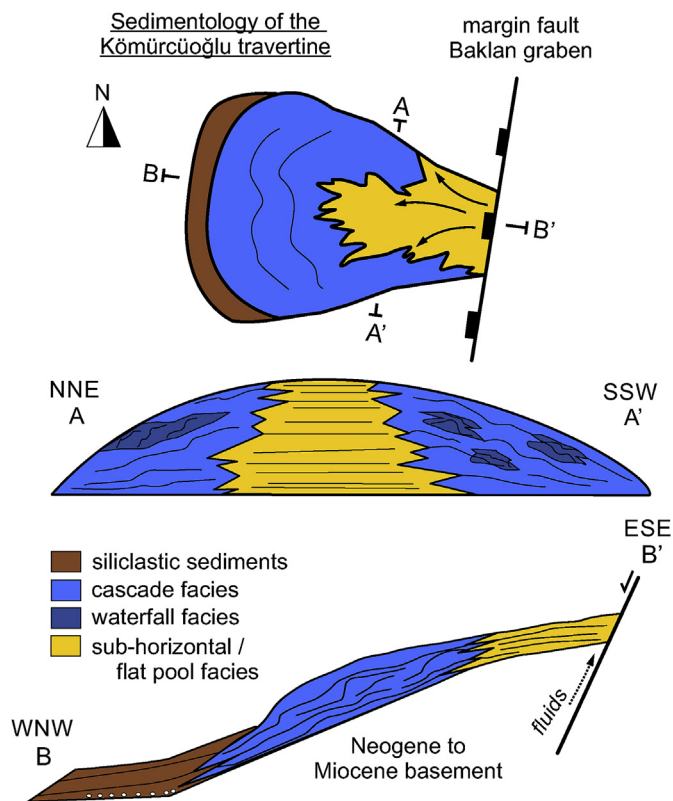
Fig. 13. Simplified conceptual model and cross-sections of the geometry of the main travertine lobe of the Kömürcüoğlu travertine. Based on the lobe geometry, a travertine source WNW of the quarry is expected.

products of cohesive debris flows (cf. Nemec and Steel, 1984).

The paleo-springs as source of the Kömürcüoğlu mound geobody should be found northeast of the Kömürcüoğlu quarry. Because the travertine geobody formed in alignment with the NE-SW trending fault system on the front of the fault-controlled Malıdağı mountain (Fig. 1), it is plausible that this fault, which is related to Baklan Graben development, acted as a source. Also north of Kömürcüoğlu (Fig. 1), the Belevi travertine system developed downslope and was sourced by the NE-SW trending graben-edge fault of the Baklan Graben (Claes et al., 2017b).

The travertine in the Killik domal area originated from meteoric fluids that have interacted with basement rocks at depth and emerged along the graben margin faults to the surface (Claes et al., 2015; El Desouky et al., 2015). The Killik dome is a depositional dome with horizontal to subhorizontal bedded travertine present in the lower part that gradually changes upwards to cascade/slope and waterfall facies travertine.

Travertine masses developed along the northern graben flank, i.e. the Pamukkale-Gama, Karakurt-Stone Terroir, Özaş, Emek-Lower Tuna and Taşkestik-Kepez Tepe travertines consist of WNW-ESE oriented (sub-)horizontal to gently S-wards sloping travertine masses (similar to the 'eroded-sheet travertines' of Altunel, 1994). As this subhorizontal travertine facies occurs north (footwall) and south (hangingwall) of the Düzçalı fault, a similar large normal fault system should be present at depth north of Düzçalı sourcing the necessary fluids for the large-scale observed subhorizontal travertine system. The extent of this fault system is unknown and can be hidden in the underlying Neogene unconsolidated sediments. Moreover, sourcing potentially also occurred diffuse through the underlying unconsolidated sediments next to fluid transport along the faults. The latter interpretation is supported by the fact that no banded travertines or central feeder system has been found in the Ballık area, thus suggesting a large depression as depositional environment (Fig. 14A). The good rock quality of the travertine masses

in the upper part suggests that at the time of travertine deposition, already an uplifted mountain morphology must have been present to create subhorizontal to slope-dominated travertine facies that were not totally destroyed by further uplift of the mountain flank.

The fact that many siliciclastic sequences intercalate and cover (Fig. 14B) the different travertine masses along the northern margin suggests that a clastic source of sediments must have been located in the mountain range north of the Ballık area (Fig. 1). However, as the Taşkestik Tepe travertine is currently the highest point in the Ballık area, a considerable uplift of the Taşkestik Tepe occurred during the late Pleistocene-Holocene (Fig. 14C) shutting of the Ballık area from this clastic source.

6.2. A relative travertine age model

Geomorphological evidence, travertine architecture and fault intersection relationships can be used to constrain an enigmatic relative travertine age model (Fig. 14). Around the world numerous examples are known (e.g. Turkey, Hungary, off shore Brazil) in which inactive travertines are present at elevated topographic levels, because they were cut off from the main water table due to tectonic uplift, and where active spring travertine precipitation has shifted to lower areas (e.g. González-Martín et al., 1989; Capezzuoli et al., 2010; Özkul et al., 2010; Özkul et al., 2013; Çolak Erol et al., 2015; Claes et al., 2017a; Wang et al., 2017). This also occurred in the DGHS as the Killik dome is younger than the travertine developed along the northern margin flank. Formation of the Killik dome occurred simultaneously when extensional deformation was affecting the already deposited travertine masses along the margin flank (Fig. 14C). Lebatard et al. (2014) concluded from paleomagnetism in combination with cosmogenic nuclide dating that the travertine in the lower part of the Killik dome ranges between 1.7 and 1.1 Ma. The younger, upper parts date between 1.22 and 1.07 Ma (Lebatard et al., 2014) but might have younger ages as the uppermost levels have not been dated yet. The Taşkestik Tepe lies 260 m higher than the youngest part of the Killik dome. Taking a slow general uplift rate of 0.2 mm/a in Anatolia (Westaway et al., 2003) into account, then the earliest deposition along the Taşkestik Tepe could potentially date back to 2.5 Ma, i.e. Early Pleistocene (Fig. 14A). This age is underestimated as erosion rates along the northern graben flank are not known/taken into account in this calculation. Erosion rates can vary substantially according to position of the area relative to the active faults and can be high along steep normal fault systems (> 330 mm/ka, see Buscher et al., 2013). Despite this overestimation, this time estimation sets a minimum possible age in which the oldest travertine deposition at Taşkestik Tepe needs to be framed.

U/Th depositional ages of the Kömürcüoğlu and Belevi travertines vary between 490 ± 50 and 510 ± 50 ka (Özkul et al., 2004), which is significantly younger than the Ballık travertine. Because both travertine masses are sourced from Baklan margin faults, this age suggest that the NE-SW 'Baklan' extensional stress regime must have been active during deposition of these travertine masses (Fig. 14D). With time the travertine deposition migrated from the northern graben flank to a more central part of the DGHS, e.g. at Koçabas (181 ka to 80 ka; Toker et al., 2014) (Fig. 14E).

6.3. Development of the Early Pleistocene extensional fault/fracture network

In Western Anatolia, the Baklan, Acigöl, Dinar, Burdur and Denizli Basins (see Fig. 1) are all characterised by master border faults that progressively young and downtrow towards the depocentre in the basin (e.g. Alçiçek et al., 2013). At Pamukkale, along the northern margin of the Denizli Basin, travertine occurrences are mainly associated to transfer zones between the stepwise NW-trending margin faults (Alçiçek et al., 2013; Kaypak and Gökkaya, 2012) in which travertine also youngs towards the basin centre, a process which is accompanied
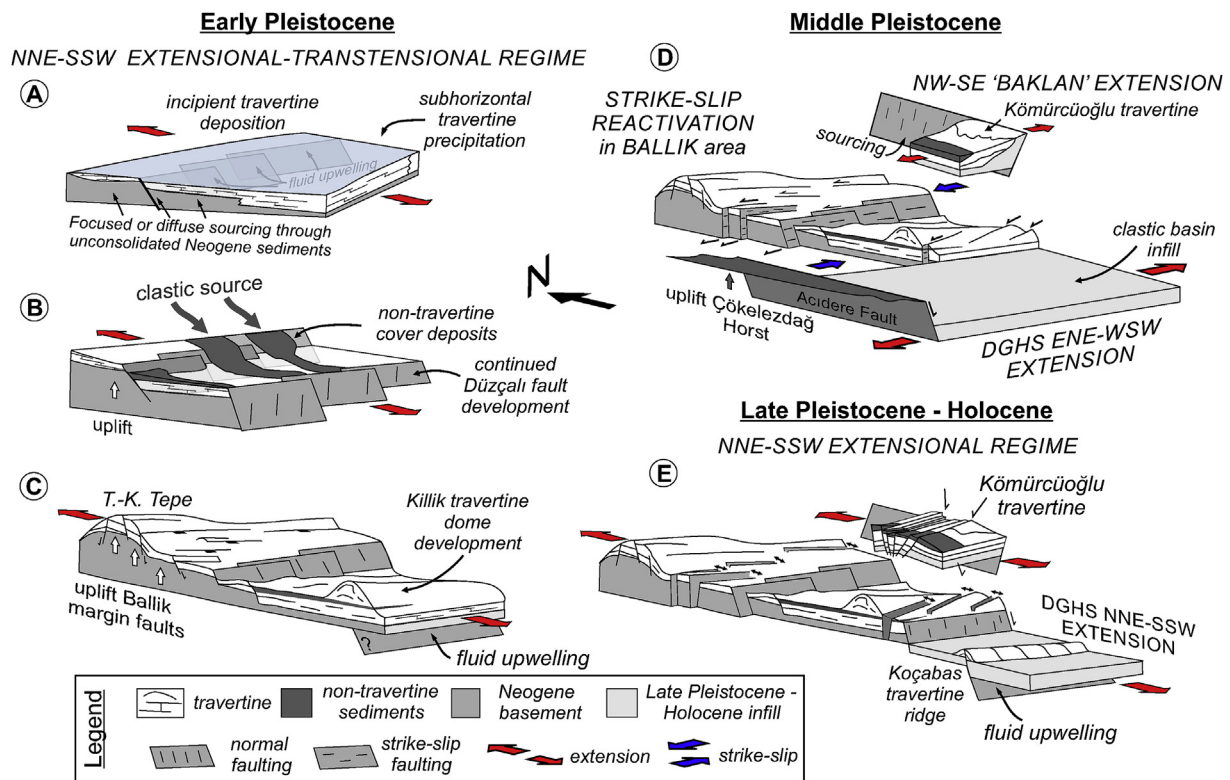
Fig. 14. Conclusive cartoon (not to scale) illustrating the sedimentological and tectonic evolution of the Ballık travertine. **A)** Early Pleistocene subhorizontal travertine development on top of Neogene basement sediments/rocks. **B)** Alluvial system covering the travertine with marly and clayey sediments sourced from the mountain range north of the Ballık area. **C)** Normal faulting and uplift of the Taşkestik (T.-K) Tepe simultaneously with development of the Killik travertine dome. **D)** Kömürcuoğlu travertine development, sourced by the NNE-SSW-trending Baklan margin fault. Baklan Graben and the DGHS in ENE-WSW extension. Normal faults in the Ballık area are reactivated into strike-slip with Ballık area acting as transfer zone. **E)** Collapse of the Ballık area with further opening and infill of normal faults. Active travertine precipitation is occurring further basin-inwards e.g. at Koçabas.

by the development of different fluvial terraces (Özkul et al., 2013). In the Ballık area, faults progressively young from the uplifted horst towards the basin centre. Hence, the paleostress regimes deduced from fault kinematica from old (upper area) to young (lower area) can be used to reconstruct the Neogene-Quaternary deformation history of the Ballık area.

Because the Quaternary travertines developed on loose Neogene sedimentary basin fills, there is however a risk that the mapped faults do not resemble the regional tectonics. Indeed, some suspicious stress inversion results and few local right-lateral fault movements (Fig. 10, Best quarry) do not resemble the regional inversions but highlight rather local tectonic features (e.g. NW-SE extension in the Kömürcuoğlu small quarry (Fig. 12) linked to gravitational collapse along the Killik fault). Unfortunately, because there are no Neogene basement outcrops in the Ballık area, the proposed tectonic model proposed in Fig. 14 cannot be verified by the substratum deformation. The majority of the stress inversions (Fig. 12), however, all result in very similar stress regimes suggesting that the analysed tectonic stress directions are regional.

From the Kepez Tepe quarry in the West to the Pamukkale quarry in the East, the WNW-ESE-oriented travertine masses are not continuous but are distributed in an en-echelon configuration (Fig. 2). This suggests that the underlying, uppermost blind margin faults, that provided the necessary fluids for travertine precipitation, also have such a configuration. Most faults cutting these subhorizontal to tilted travertine masses in the upper Ballık area are WNW-ESE oriented and are slightly obliquely oriented to margin-bounding faults such as the Düzçalı and Killik faults, which show a segmented, en-echelon configuration. Paleostress analysis on faults cutting the en-echelon arranged travertine masses in the upper Ballık area indicates that fault segmentation

developed during a NNE-SSW oriented extensional-transtensional stress regime (Figs. 12 and 14A–C) during the Early Pleistocene (see section 6.2). The dense and often fault-parallel joint network indicates that faulting in the Early Pleistocene was accompanied by fracturing. In the Kömürcuoğlu quarry, joints and faults in the northern part dip steeply to the south whereas joints and faults in the southern part dip moderately to the north. This parallelism would not be present if jointing would post-date faulting. Due to the shallow burial, tensile Mode I fractures dominate the deformation in the Ballık area. The alignment and consistent orientation of joints and extension veins contribute to the interpretation of the paleostress results as Mode I fractures open perpendicular to minimum principal stress direction (σ_3), both at shallow (Laubach et al., 2004) or at large depths (Van Noten et al., 2012).

6.4. Middle Pleistocene strike-slip tectonics

In the middle and lower Ballık area, the muddy fault infill and secondary cementation phases are often striated by subhorizontal slickenlines, interpreted as strike-slip reactivation features. Stress inversion of the Ballık strike-slip fault reactivation data results in an ENE-WSW oriented σ_1 (compression) and NNW-SSE oriented σ_3 (extension) (Fig. 12). The strike-slip tectonic stress regime that caused this reactivation clearly post-dates the previous NNE-SSW extensional phase as strike-slip markers are always observed on normal fault infills and hardly ever as mechanical striations directly on the fault walls. The particular strike-slip stress orientation is the proper orientation to activate the NNE-SSW Baklan margin faults as normal faults (a process further noted as 'Baklan' extension). Hence, the parallelism of σ_1 in the strike-slip regime of the Ballık area with σ_3 during 'Baklan' extension

strongly suggests that the 'Baklan' extension can be interpreted as the driving force to reactivate the ENE-WSW fault network in the Ballık area. When NW-SE 'Baklan' extension affected the DGHS, the NNE-trending Acıdere fault east of the Ballık area (Figs. 2 and 14) was also favourably oriented to be reactivated as an oblique normal fault (Koçyiğit, 2005) causing subsidence of the Denizli Basin floor and uplift of the footwall, i.e. the Çökelezdağ Horst (Fig. 14D). At the time when 'Baklan' extension affected the Acıdere fault, the inherited WNW-ESE Ballık fault network thus acted as border faults for this extension and was, given its favourable orientation, reactivated into sinistral strike-slip faults. The Ballık area can thus be considered as a strike-slip transfer zone (Fig. 14D) from the Acidere fault to the western border fault of the Baklan Basin. To which extent additional travertine formation (and fluid flow) is related to localised extension along the Ballık transfer zone due to sinistral reactivation of the left-stepping normal fault system (cf. Rotevatn and Peacock, accepted) is unknown.

The stress change from Early Pleistocene extension to Middle Pleistocene strike-slip involved reorientation of the stress axes in which σ_1 switched to horizontal and σ_2 and σ_3 switched from regional NNE-SSW Denizli extension to regional NW-SE to WNW-ESE 'Baklan' extension. These stress permutations may easily occur as close to the Earth's surface differential stresses are low (Hancock and Engelder, 1989) and differences in principal stress magnitudes are small. Moreover, in a fault network, faults tend to involve reactivation of existing faults rather than creating new faults (Scholz, 1998), especially if the fault orientation is in an optimum angle for reactivation (Sibson, 1985).

The Kömürcüoğlu, Gama and Pamukkale travertine masses are preserved from strike-slip faulting. They are situated at the southern end of the Baklan Graben and are thus excluded from the transfer zone and hence neither strike-slip faults nor any NE-SW trending joints affected these quarries. Also along the Kepez and Taşkestik Tepe, no strike-slip features are observed as these travertine masses were already uplifted along the margin shoulders and were protected from reactivation. Additional proof of the interaction of the Baklan Basin with the Denizli Basin is given by Kaymakçı (2006) who proved that sharp changes occur around subsurface lineaments in the DGHS at places where major basin geometrical changes occur. The change in basin geometry from E to W orientation between Gürleyik and Honaz to a NW to SE orientation between Kocabaş and Ballık (Fig. 2) shows that the NW-SE extension of the neighbouring Baklan Graben strongly contributed to the evolution of the eastern DGHS.

6.5. Late Pleistocene – Holocene extension

During the late Pleistocene – Holocene considerable block tilting has taken place. The NNE-dipping travertine observed in the Reisoğlu-Özaş, Emek, Lower Tuna, Kepez and Taşkestik Tepe and Cinkaya quarries (Figs. 7–10) are examples of block tilting as travertine in the hangingwall is tilted northwards towards the footwall as a result of normal faulting. Another example of block tilting occurs in the southern part of the Emek, Kepez and Taşkestik Tepe quarries where travertine in the hangingwall of normal faults dips towards the Denizli Basin to the SSW (Figs. 7C–C′ and 11F-F′).

Many faults along the northern flank are filled by clayey and marly sediments, either by gravitational of hydrological transport, and calcite cementation along the fault walls is common. The sedimentary infill, open nature of the faults, various fracture patterns and dissolution-enlarged fractures are typical for shallow dilatant fault zones developed along already uplifted extensional graben shoulders (van Ghendt et al., 2010). Fault widening and infill is observed along both strike-slip reactivated and normal faults and can be related to the Late Pleistocene – Holocene deformation stage (Fig. 14E).

The fact that all faults in the Killik dome abut against Killik Fault, suggests that the latest activity in Ballık area took place along the Killik fault. After all, alluvial Quaternary sediments are deposited in the Denizli Basin floor in the hangingwall of the Killik fault. The left-lateral

stepwise orientation of the Killik fault moreover suggests that a transtensional component was still present in the late-Pleistocene to Holocene causing further oblique opening in this part of the DGHS. Finally, active extension and related travertine precipitation took place further basin inwards as illustrated by several travertine ridges at e.g. Kocabaş.

Focal mechanisms of recent earthquakes (Taymaz and Price, 1992; Price and Scott, 1994; Gürbüz et al., 2012; Kaypak and Gökkaya, 2012; Irmak, 2013), geodetic data, south-westwards GPS-based vectors (Elitez and Yaltırak, 2016) and stress indicators on the World Stress Map (e.g. N23E extension for the M_L 4.8 20080425 earthquake at Gürleyik, Fig. 1) all indicate that current extension is still NNE-SSW in the eastern DGHS.

6.6. Strike-slip reactivation at graben intersections

Large stress reconfigurations driving graben development and subsequent fault reactivation are also recognised along the Dinar transfer zone (Fig. 1B). The Baklan, Acigöl and Burdur halfgrabens are all bounded by major NW-dipping normal faults and are considered to have initiated parallel to the Dinar transfer zone during the late Miocene-Pliocene in a NW-SE oriented extensional phase (Westaway, 1990). Further development and NE-SW opening of the Dinar Basin in the Quaternary resulted in sinistral oblique-slip reactivation of the NW-normal faults bounding the Baklan, Acigöl and Burdur Basins, due to differential stretching of the inner blocks on top of the Dinar fault zone (Westaway, 1990; Verhaert et al., 2006; Gürbüz et al., 2012; Alçiçek et al., 2013).

With exception of the Ballık area, large-scale strike-slip faulting has hardly ever been observed in the DGHS. The only mappable strike-slip faults are a NW-trending strike-slip fault at Hierapolis offsetting a historic man-made channel (Altunel and Hancock, 1993b) and two closely-spaced faults affecting the Upper Miocene ancient basin fill in the Alikurt area in the easternmost Kaklık area (see the opposite facing-faults at Alikurt in the eastern part of Fig. 2). Kinematic analysis in the Alikurt area indicates a Middle Pliocene strike-slip regime with ENE-WSW compression post-dating an earlier regional NNE-SSW extension phase (Koçyiğit, 2005). As this Middle Pliocene strike-slip phase predates Ballık travertine precipitation, it shows that during the entire development of the DGHS transient periods of regional stress reconfigurations have taken place at its borders due to the tectonic influence of adjacent basins. It is thus concluded that in the Ballık area, a dense fault/fracture network was formed due to interaction of the DGHS and Baklan Basin extensional tectonics. This strongly enhanced fluid flow from which large travertine geobodies formed.

7. Conclusions

Detailed structural mapping of neotectonic faults and fractures and an evaluation of the Ballık travertine geodynamic evolution lead to a reconstruction of the kinematic deformation history of the eastern part of the Denizli Graben-Horst System in SW Turkey. This study demonstrates the importance of incorporating tectonic fault analyses into travertine geobody reconstructions to understand the geodynamic history of continental carbonates. Based on the detailed tectonic analysis and paleostress inversion carried out on fault-slip data gathered from 35 quarries, the following conclusions can be drawn:

1) The Ballık travertine is deformed by WNW-ESE-oriented normal faults that are either parallel or slightly oblique to the Düzçalı and Killik incipient margin-bounding faults.
2) The upper part of the margin was only affected by extension and is marked by backtilted travertine in the hangingwall of normal faults. Paleostress inversion shows that travertine precipitation and subsequent emplacement of the fault network took place during a long-lived phase of NNE-SSW extension in the Early Pleistocene. Block

tilting, back rotation, fault infill, secondary fluid flow and extensional fracturing, creating a dense joint network, accompanied faulting during this stress state.

3) Both in the footwall and in the hangingwall of the Düzçalı fault, and in the lower Killik dome, WNW-ESE normal faults are reactivated into sinistral strike-slip faults. Reactivation is evidenced by strike-slip slickenlines that are mostly developed on the muddy fault infill and on polished surfaces of secondary cement infill. The sinistral reactivation of normal faults corresponds to a strike-slip regime with NE-SW to ENE-WSW compression and NW-SE to NNW-SSE extension in the Ballık area. This phase can be related to a NW-SE extensional stress-state during which the NNE-SSW border faults of the Baklan Graben were in extension and during which the edge of the eastern part of the DGHS, i.e. the Acıdere fault, was favourably oriented to be reactivated. The Ballık area acted as a transfer zone in this period.

4) A NNE-SSW extensional phase reinstalled in the late Pleistocene-Holocene causing further fault widening and clastic fault infill in the Ballık area and active travertine deposition in the central part of the DGHS. This stress state is currently still active.

5) Large travertine deposits are likely to develop at graben intersections because of the presence of an underground fault-fracture network that can be formed during different tectonic regimes. Graben intersections are therefore susceptible to an enhanced fluid flow induced by stress permutations and fault reactivation.

6) Based on fault distribution of the Killik dome it is concluded that large domes have a large rigidity with fault development affecting preferentially its flanks but hardly its centre.

7) Faults developed at the intersection of different extensional graben structures can easily reactivate due to stress reconfigurations, whereas this is less common in the middle of such grabens.

Data availability

Fault orientations and fault names, quarry locations and observation points are included as a Google Earth™ kml file in Suppl. Mat. S1. A coordinate list of quarry locations is available in S2. All fault and fracture orientation data are provided as *.csv files in S3. Detailed descriptions of the quarries are presented in S4. The datasets can also be consulted at Mendeley Data (Van Noten, 2018).

Acknowledgements

Appendix A. Supplementary data

Supplementary data associated with this article can be found, in the online version, at https://doi.org/10.1016/j.jsg.2018.10.009.

References

Alçiçek, H., Varol, B., Özkul, M., 2007. Sedimentary facies, depositional environments and palaeogeographic evolution of the Neogene Denizli Basin, SW Anatolia, Turkey. Sediment. Geol. 202 (4), 596–637.
Alçiçek, M.C., Brogi, A., Capezzuoli, E., Liotta, D., Meccheri, M., 2013. Superimposed basin formation during neogene–quaternary extensional tectonics in SW-Anatolia (Turkey): insights from the kinematics of the Dinar fault zone. Tectonophysics 608, 713–727.
Altunel, E., 1994. Active Tectonics and the Evolution of Quaternary Travertines at Pamukkale. PhD thesis. University of Bristol, Western Turkey, pp. 236.
Altunel, E., Hancock, P.L., 1993a. Active fissuring and faulting in Quaternary travertines at Pamukkale, western Turkey. Z. Geomorph. NF 94, 285–302.
Altunel, E., Hancock, P.L., 1993b. Morphology and structural setting of Quaternary travertines at Pamukkale, western Turkey. Geol. J. 28, 335–346.
Altunel, E., Hancock, P.L., 1996. Structural attributes of travertine-filled extensional fissures in the Pamukkale plateau, western Turkey. Int. Geol. Rev. 38 (8), 768–777.
Altunel, E., Karabacak, V., 2005. Determination of horizontal extension from fissure-ridge travertines: a case study from the Denizli Basin, southwestern Turkey. Geodin. Acta 18 (3–4), 333–342.
Angelier, J., Mechler, P., 1977. Sur une méthode graphique de recherche des contraintes principales également utilisable en tectonique et en séismologie: la méthode des dièdres droits. Bull. Soc. Geol. Fr. 7 (6), 1309–1318.
Bott, M.P.H., 1959. The mechanics of oblique-slip faulting. Geol. Mag. 96, 109–117.
Bozkurt, E., 2001. Neotectonics of Turkey - a synthesis. Geodin. Acta 14, 3–30.
Bozkurt, E., Sözbilir, H., 2006. Evolution of the large-scale Active manisa fault, southwest Turkey: implications on fault development and regional tectonics. Geodin. Acta 19 (6), 427–453.
Brogi, A., 2004. Faults linkage, damage rocks and hydrothermal fluid circulation: tectonic interpretation of the Rapolano Terme travertines (southern Tuscany, Italy) in the context of Northern Apennines Neogene–Quaternary extension. Eclogae Geol. Helv. 97, 307–320.
Brogi, A., Capezzuoli, E., 2009. Travertine deposition and faulting: the fault-related travertine fissure-ridge at Terme S. Giovanni, Rapolano Terme (Italy). Int. J. Earth Sci. 98, 931–947.
Brogi, A., Capezzuoli, E., 2014. Earthquake impact on fissure-ridge type travertine deposition. Geol. Mag. Rapid Commun. 1–9.
Brogi, A., Capezzuoli, E., Alçiçek, M.C., Gandin, A., 2014. Evolution of a fault-controlled fissure-ridge type travertine deposit in the western Anatolia extensional province: the Çukurbağ fissure-ridge (Pamukkale, Turkey). J. Geol. Soc. 171 (3), 425–441.
Brogi, A., Capezzuoli, E., Aqué, R., Branca, M., Voltarrio, M., 2010. Studying travertine for neotectonic investigations: middle-Late Pleistocene syn-tectonic travertine deposition at Serra di Rapolano (Northern Apennines, Italy). Int. J. Earth Sci. 99, 1383–1398.
Brogi, A., Capezzuoli, E., Buracchi, E., Branca, M., 2012. Tectonic control on travertine and calcareous tufa deposition in a low-temperature geothermal system (Sarteano, Central Italy). J. Geol. Soc. 169 (4), 461–476.
Brogi, A., Alçiçek, M.C., Yalçıner, C.Ç., Capezzuoli, E., Liotta, D., Meccheri, M., Rimondi, V., Ruggieri, G., Gandin, A., Boschi, C., Büyüksaraç, A., Alçiçek, H., Bülbül, A., Baykara, M.O., Shen, C.-C., 2016. Hydrothermal fluids circulation and travertine deposition in an active tectonic setting: insights from the Kamara geothermal area (western Anatolia, Turkey). Tectonophysics 680, 211–232.
Buckley, J.P., Elders, C., Mann, J., 2013. Carbonate buildups in the santos basin, offshore Brazil. Programme and abstract volume: microbial Carbonates in Space and time: Implications for global Exploration and production. In: The Geological Society. 19 – 20 June, 2013.
Buscher, J.T., Hampel, A., Hetzel, R., Dunkl, I., Glotzbach, C., Struffert, A., Akal, C., Rätz, M., 2013. Quantifying rates of detachment faulting and erosion in the central Menderes Massif (western Turkey) by thermochronology and cosmogenic 10Be. J. Geol. Soc. 170 (4), 669–683.
Çakır, Z., 1999. Along-strike discontinuities of active normal faults and its influence on Quaternary travertine deposition; examples from western Turkey. Turk. J. Earth Sci. 8, 67–80.
Capezzuoli, E., Gandin, A., Sandrelli, F., 2010. Calcareous tufa as indicators of climatic variability: a case study from southern Tuscany (Italy). Geol. Soc. Lond. Spec. Publ. 336 (1), 263–281.
Çelik, S., Çobanoğlu, İ., Atatanır, L., 2014. General material properties of Denizli (SW Turkey) travertines as a building stone. Bull. Eng. Geol. Environ. 73 (3), 825–838.
Çiftçi, N.B., Bozkurt, E., 2009. Pattern of normal faulting in the Gediz graben, SW Turkey. Tectonophysics 473 (1–2), 234–260.
Claes, H., Degros, M., Soete, J., Claes, S., Kele, S., Mindszenty, A., Török, Á., El Desouky, H., Vanhaecke, F., Swennen, R., 2017a. Geobody architecture, genesis and petrophysical characteristics of the Budakalász travertines, Buda Hills (Hungary). Quat. Int. 437, 107–128.
Claes, H., Erthal, M., Soete, J., Özkul, M., Swennen, R., 2017b. Shrub and pore type classification: petrography of travertine shrubs from the Ballık-Belevi area (Denizli, SW Turkey). Quat. Int. 437, 147–163.
Claes, H., Soete, J., Van Noten, K., El Desouky, H., Marques Erthal, M., Vanhaecke, F., Özkul, M., Swennen, R., 2015. Sedimentology, three-dimensional geobody reconstruction and carbon dioxide origin of Pleistocene travertine deposits in the Ballık area (south-west Turkey). Sedimentology 62, 1408–1445.
Çobanoğlu, I., Çelik, S.B., 2012. Determination of strength parameters and quality assessment of Denizli travertines (SW Turkey). Eng. Geol. 129–130, 38–47.
Çolak Erol, S., Özkul, M., Aksoy, E., Kele, S., Ghaleb, B., 2015. Travertine occurrences along major strike-slip fault zones: structural, depositional and geochemical constraints from the Eastern Anatolian fault System (EAFS), Turkey. Geodin. Acta. https://doi.org/10.1080/09853111.2014.979530.
De Boever, E., Foubert, A., Lopez, B., Swennen, R., Jaworowski, C., Özkul, M., Virgone, A., 2017. Comparative study of the Pleistocene Cakmak quarry (Denizli basin,Turkey) and modern mammoth hot springs deposits (yellowstone national park, USA). Quat. Int. 437, 129–146.
De Boever, E., Foubert, A., Oligschlaeger, D., Claes, S., Soete, J., Bertier, P., Özkul, M.,

Virgone, A., Swennen, R., 2016. Multiscale approach to (micro)porosity quantification in continental spring carbonate facies: case study from the Cakmak quarry (Denizli, Turkey). G-cubed 17 (7), 2922–2939.

De Filippis, L., Faccenna, C., Billi, A., Anzalone, E., Brilli, M., Özkul, M., Soligo, M., Tuccimei, P., Villa, I.M., 2012. Growth of fissure ridge travertines from geothermal springs of Denizli Basin, western Turkey. Geol. Soc. Am. Bull. 124, 1629–1645.

De Filippis, L., Faccenna, C., Billi, A., Anzalone, E., Brilli, M., Soligo, M., Tuccimei, P., 2013. Plateau versus fissure ridge travertines from Quaternary geothermal springs of Italy and Turkey: interactions and feedbacks between fluid discharge, paleoclimate, and tectonics. Earth Sci. Rev. 123 (0), 35–52.

Delvaux, D., Sperner, B., 2003. Stress tensor inversion from fault kinematic indicators and focal mechanism data: the TENSOR program. In: In: Nieuwland, D. (Ed.), New Insights into Structural Interpretation and Modelling, vol. 212. Geological Society, London, Special Publications, pp. 75–100.

El Desouky, H., Soete, J., Claes, H., Özkul, M., Vanhaecke, F., Swennen, R., 2015. Novel applications of fluid inclusions and isotope geochemistry in unravelling the genesis of fossil travertine systems. Sedimentology 62 (1), 27–56.

Elitez, İ., Yaltırak, C., 2016. Miocene to Quaternary tectonostratigraphic evolution of the middle section of the Burdur-Fethiye Shear Zone, south-western Turkey: implications for the wide inter-plate shear zones. Tectonophysics 690, 336–354.

Faccenna, C., 1994. Structural and hydrogeological features of Pleistocene shear zones in the area of Rome (Central Italy). Ann. Geofica 37 (1), 121–133.

Faccenna, C., Soligo, M., Billi, A., De Filippis, L., Funiciello, R., Rossetti, C., Tuccimei, P., 2008. Late Pleistocene depositional cycles of the Lapis Tiburtinus travertine (Tivoli, Central Italy): possible influence of climate and fault activity. Global Planet. Change 63 (4), 299–308.

Faulds, J.E., Bouchot, V., Moeck, I., Oguz, K., 2009. Structural controls on geothermal systems in Western Turkey: a preliminary report. Trans. Geoth. Resour. Counc. 33, 375–381.

Gessner, K., Gallardo, L.A., Markwitz, V., Ring, U., Thomson, S.N., 2013. What caused the denudation of the Menderes Massif: review of crustal evolution, lithosphere structure, and dynamic topography in southwest Turkey. Gondwana Res. 24 (1), 243–274.

Gessner, K., Markwitz, V., Güngör, T., 2017. Crustal Fluid Flow in Hot Continental Extension: Tectonic Framework of Geothermal Areas and Mineral Deposits in Western Anatolia. Geological Society, London, Special Publications, 453 SP453–7.

González-Martín, J.A., García del Cura, M.A., Ordóñez, S., 1989. Formaciones tobaceas en los valles Tajuña y Tajo. In: Excursion Guide C-4. Reunion del Cuaternario Iberico, Madrid 25–29 September 1989. Association of Española Estudio del Cuaternario (AEQUA) – Grupo Trabalho Portugies Estudodo Quaternario (GTPEQ).

Güleç, N., Hilton, D.R., Mutlu, H., 2002. Helium isotope variations in Turkey: relationship to tectonics, volcanism and recent seismic activities. Chem. Geol. 187, 129–142.

Gürbüz, A., Boyraz, S., Ismael, M.T., 2012. Plio-Quaternary development of the Baklan–Dinar graben: implications for cross-graben formation in SW Turkey. Int. Geol. Rev. 54 (1), 33–50.

Hancock, P.L., Chalmers, R.M.L., Altunel, E., Çakir, Z., 1999. Travitonics: using travertines in active fault studies. J. Struct. Geol. 21, 903–916.

Hancock, P.L., Engelder, T., 1989. Neotectonic joints. Geol. Soc. Am. Bull. 101 (10), 1197–1208.

Irmak, S., 2013. Focal mechanisms of small-moderate earthquakes in Denizli Graben (SW Turkey). Earth Planets Space 65, 943–955.

Irmak, S., Taymaz, T., 2009. Source mechanics of recent moderate earthquakes occurred in Honaz-Denizli (W Turkey) graben obtained by regional broadband waveform inversion. In: International Symposium on Historical Earthquakes and Conservation of Monuments in the Eastern Mediterranean Region, Istanbul, Turkey, pp. 350–356.

Kaymakçı, N., 2006. Kinematic development and paleostress analysis of Denizli Basin (W Turkey): implications of spatial variation of relative paleostress magnitudes and orientations. J. Asian Earth Sci. 27, 207–222.

Kaypak, B., Gökkaya, G., 2012. 3-D imaging of the upper crust beneath the Denizli geothermal region by local earthquake tomography, western Turkey. J. Volcanol. Geoth. Res. 211–212, 47–60.

Kele, S., Demény, A., Siklósy, Z., Németh, T., Tóth, M., Kovács, M.B., 2008. Chemical and stable isotope composition of recent hot-water travertines and associated thermal waters, from Egerszalók, Hungary: depositional facies and non-equilibrium fractionation. Sediment. Geol. 211 (3–4), 53–72.

Kele, S., Özkul, M., Fórizs, I., Gökgöz, A., Baykara, M.O., Alçiçek, M.C., Németh, T., 2011. Stable isotope geochemical study of Pamukkale travertines: new evidences of low-temperature non-equilibrium calcite-water fractionation. Sediment. Geol. 238 (1–2), 191–212.

Khatib, S., Rochette, P., Alçiçek, M.C., Lebatard, A.-E., Demory, F., Saos, T., 2014. Études stratigraphique, sédimentologique et paléomagnétique des travertins de Kocabaş, Bassin de Denizli, Anatolie, Turquie, contenant des restes fossiles quaternaires. L'Anthropol. 118 (1), 16–33.

Kipata, M.L., Delvaux, D., Sebagenzi, M.N., Cailteux, J., Sintubin, M., 2013. Brittle tectonic and stress field evolution in the Pan-African Lufilian arc and its foreland (Katanga, DRC): from orogenic compression to extensional collapse, transpressional inversion and transition to rifting. Geol. Belg. 16 (1–2), 1–17.

Koçyiğit, A., 2005. The Denizli graben-horst system and the eastern limit of western Anatolian continental extension: basin fill, structure, deformational mode, throw amount and episodic evolutionary history, SW Turkey. Geodin. Acta 18 (3–4), 167–208.

Laubach, S.E., Olson, J.E., Gale, J.F.W., 2004. Are open fractures necessarily aligned with maximum horizontal stresses? Earth Planet Sci. Lett. 222, 191–195.

Lebatard, A.-E., Alçiçek, M.C., Rochette, P., Khatib, S., Vialet, A., Boulbes, N., Bourlès, D.L., Demory, F., Guipert, G., Mayda, S., Titov, V.V., Vidal, L., de Lumley, H., 2014. Dating the Homo erectus bearing travertine from Kocabaş (Denizli, Turkey) at at least 1.1 Ma. Earth Planet Sci. Lett. 390, 8–18.

Loveless, S., Bense, V., Turner, J., 2011. Fault architecture and deformation processes within poorly lithified rift sediments, Central Greece. J. Struct. Geol. 33 (11), 1554–1568.

Maggi, M., Cianfarr, P., Salvini, F., Coelho de Lima, C., 2015. Staircase fractures in microbialites and the role of lamination-related mechanical anisotropy: the example of the Acquasanta Terme travertine deposits (Central Italy). GSA Bull. 127, 879–896.

Martínez-Díaz, J.J., Hernández-Enrile, J.L., 2001. Using travertine deformations to characterize paleoseismic activity along an active oblique-slip fault: the Alhama de Murcia fault (Betic Cordillera, Spain). Geol. Acta 36 (3–4), 297–313.

McKenzie, D., 1970. The plate tectonics of the Mediterranean region. Nature 226, 239–243.

Mesci, B.L., Gursoy, H., Tatar, O., 2008. The evolution of travertine masses in the sivas area (Central Turkey) and their relationships to active tectonics. Turk. J. Earth Sci. 17, 219–240.

Nemec, W., Steel, R.J., 1984. Alluvial and coastal conglomerates: their significant features and some comments on gravelly mass-flow deposits. Sedimentol. Gravels Conglom. 10, 1–31.

Özkaymak, Ç., 2015. Tectonic analysis of the Honaz Fault (western Anatolia) using geomorphic indices and the regional implications. Geodin. Acta 27 (2–3), 110–129.

Özkul, M., Engin, B., Alçiçek, M.C., Koralay, T., Demirtaş, H., 2004. Thermoluminescence dating of Quaternary hot spring travertines and some implications on graben evolution, Denizli, Western Turkey. In: 32nd International Geological Congress, August 20–28, 2004, Florence, Italy.

Özkul, M., Gökgöz, A., Horvatinčíć, N., 2010. Depositional properties and geochemistry of Holocene perched springline tufa deposits and associated spring waters: a case study from the Denizli Province, Western Turkey. Geol. Soc. Lond. Spec. Publ. 336 (1), 245–262.

Özkul, M., Gökgöz, A., Kele, S., Baykara, M.O., Shen, C.-C., Chang, Y.-W., Kaya, A., Hançer, M., Aratman, C., Akin, T., Örü, Z., 2014. Sedimentological and geochemical characteristics of a fluvial travertine: a case from the eastern Mediterranean region. Sedimentology 61 (1), 291–318.

Özkul, M., Kele, S., Gökgöz, A., Shen, C.-C., Jones, B., Baykara, M.O., Fórizs, I., Németh, T., Chang, Y.-W., Alçiçek, M.C., 2013. Comparison of the quaternary travertine sites in the Denizli extensional basin based on their depositional and geochemical data. Sediment. Geol. 294, 179–204.

Özkul, M., Varol, B., Alçiçek, M.C., 2002. Depositional environments and petrography of the Denízlí travertines. Miner. Res. Expl. Bull. 125, 13–29.

Piccardi, L., 2007. The ad 60 Denizli basin earthquake and the apparition of archangel michael at colossae (aegean Turkey). Geol. Soc. Lond. Spec. Publ. 273 (1), 95.

Price, S.P., Scott, B., 1994. Fault-block rotations at the edge of a zone of continental extension; southwest Turkey. J. Struct. Geol. 16 (3), 381–392.

Röller, K., Trepmann, C.A., 2003. Stereo32 Version 1.0.2. Ruhr Universität Bohum.

Rotevatn, A., Peacock, D.C.P. accepted. Strike-slip reactivation of segmented normal faults: Implications for basin structure and fluid flow. Basin Research. doi.org/10.1111/bre.12303.

Saller, A., Rushton, S., Buambua, L., Inman, K., McNeil, R., Dickson, J.A.D., 2016. Presalt stratigraphy and depositional systems in the Kwanza Basin, offshore Angola. AAPG Bull. 100, 1135–1164.

Scholz, C.H., 1998. Earthquakes and friction laws. Nature 391 (37–42).

Seyítoğlu, G., Scott, B.C., 1996. The cause of N-S extensional tectonics in western Turkey: tectonic escape vs back-arc spreading vs orogenic collapse. J. Geodyn. 22 (1), 145–153.

Sharp, I., Verwer, K., Ferreira, H., Lapponi, F., Snidero, M., Machado, V., Holtar, E., Swart, R., Marsh, J., Gindre, L., Puigdefabregas, C., Fejerskov, M., 2013. Pre- and post-salt non-marine carbonates of the Namibe Basin, Angola. Programme and abstract volume: microbial Carbonates in Space and time: Implications for global Exploration and production. In: The Geological Society. 19-20 June, 2013.

Sibson, R., 1985. A note on fault reactivation. J. Struct. Geol. 7 (6), 751–754.

Soete, J., Kleipool, L.M., Claes, H., Claes, S., Hamaekers, H., Kele, S., Özkul, M., Foubert, A., Reijmer, J.J.G., Swennen, R., 2015. Acoustic properties in travertines and their relation to porosity and pore types. Mar. Petrol. Geol. 59, 320–335.

Taymaz, T., Price, S., 1992. The 1971 May 12 Burdur Earthquake sequence, SW Turkey - a synthesis of seismological and geological observations. Geophys. J. Int. 108, 589–603.

Temiz, U., Gökten, Y.E., Eikenberg, J., 2013. Strike-slip deformation and U/Th dating of travertine deposition: examples from North Anatolian fault zone, bolu and yeniçağ basins, Turkey. Quat. Int. 312 (0), 132–140.

ten Veen, J.H., Boulton, S.J., Alçiçek, M.C., 2009. From palaeotectonics to neotectonics in the Neothetys realm: the importance of kinematic decoupling and inherited structural grain in SW Anatolia (Turkey). Tectonophysics 473 (1–2), 261–281.

Toker, E., Kayseri-Özer, M.S., Özkul, M., Kele, S., 2014. Depositional system and palaeoclimatic interpretations of middle to late Pleistocene travertines: Kocabaş, Denizli, south-west Turkey. Sedimentology 62, 1360–1383.

Topal, S., 2012. Denizli Havzasındaki Fayların Tektonik Jeomorfolojisi. Unpublished PhD thesis Pamukkale University 145 pp. (in Turkish with English abstract). Unpublished PhD thesis.

Topal, S., Özkul, M., 2014. Soft-sediment deformation structures interpreted as seismites in the Kolankaya formation, Denizli basin (SW Turkey). Sci. World J., 352654 13 pp.

USGS Earthquake Catalog. . https://earthquake.usgs.gov/earthquakes/search/, Accessed date: 20 September 2018.

van Ghendt, H.W., Holland, M., Urai, J.L., Loosveld, R., 2010. Evolution of fault zones in carbonates with mechanical stratigraphy - insights from scale models using layered cohesive powder. J. Struct. Geol. 32, 1375–1391.

van Hinsbergen, D.J.J., Kaymakci, N., Spakman, W., Torsvik, T.H., 2010. Reconciling the geological history of western Turkey with plate circuits and mantle tomography. Earth Planet Sci. Lett. 297 (3–4), 674–686.

Van Noten, Koen, 2018. Orientation Data of Faults and Fractures Crossing the Ballık Travertine (Denizli Basin, SW Turkey). Mendeley Data, v1. https://doi.org/10.17632/pxr49b53xn.1.

Van Noten, K., Soete, J., Claes, H., Foubert, A., Özkul, M., Swennen, R., 2013. Fracture networks and strike-slip deformation along reactivated normal faults in Quaternary travertine deposits, Denizli Basin, Western Turkey. Tectonophysics 588, 154–170.

Van Noten, K., Van Baelen, H., Sintubin, M., 2012. The complexity of 3D stress-state changes during compressional tectonic inversion at the onset of orogeny. In: Healy, D., Butler, R.W.H., Shipton, Z.K., Sibson, R.H. (Eds.), Faulting, Fracturing, and Igneous Intrusion in the Earth's Crust. vol. 367. Geological Society, London, Special Publications, pp. 51–69.

Verhaert, G., Similox-Tohon, D., Vandycke, S., Sintubin, M., Muchez, P., 2006. Different stress states in the Burdur-Isparta region (SW Turkey) since Late Miocene times: a reflection of a transient stress regime. J. Struct. Geol. 28, 1067–1083.

Wallace, R.E., 1951. Geometry of shearing stress and relation to faulting. J. Geol. 69, 118–130.

Wang, Z., Meyer, M.C., Gliganic, L.A., Hoffmann, D.L., May, J.-H., 2017. Timing of fluvial terrace formation and concomitant travertine deposition in the upper Sutlej River (Tirthapuri, southwestern Tibet) and paleoclimatic implications. Quat. Sci. Rev. 169, 357–377.

Westaway, R., 1990. Block rotation in western Turkey, 1. Observational evidence. J. Geophys. Res. 95, 19857–19884.

Westaway, R., 1993. Neogene evolution of the Denizli region of western Turkey. J. Struct. Geol. 15, 37–53.

Westaway, R., Guillou, H., Yurtmen, S., Demir, T., Scaillet, S., Rowbotham, G., 2005. Constraints on the timing and regional conditions at the start of the present phase of crustal extension in western Turkey, from observations in and around the Denizli region. Geodin. Acta 18 (3–4), 209–238.

Westaway, R., Pringle, M., Yurtmen, S., Demir, T., Bridgland, D., Rowbotham, G., Maddy, D., 2003. Pliocene and Quaternary surface uplift of western Turkey revealed by long-term river terrace sequences. Curr. Sci. 84 (8), 1090–1101.

Yalçiner, C.C., 2013. Investigation of the subsurface geometry of fissure-ridge travertine with GPR, Pamukkale, western Turkey. J. Geophys. Eng. 10, 035001 10pp.